



**ADDIS ABABA UNIVERSITY**  
**FACULTY OF TECHNOLOGY**  
**SCHOOL OF GRADUATE STUDIES**

**ANALYSIS OF STRESSES IN HELICAL GEARS**  
**BY FINITE ELEMENT METHOD**

**A thesis submitted to the School of Graduate Studies of Addis Ababa  
University in partial fulfillment of the requirement of the Degree of  
Masters of Science in Mechanical Engineering  
(Applied Mechanics Stream)**

**By  
Negash Alemu**

**Advisor  
Dr.Ing. Tamrat Tesfaye**

**October 2007**

## **Acknowledgment**

I would like to express my deep sense of gratitude towards my advisor Dr.Ing. Tamirat Tesfaye for his invaluable guidance, encouragements and inspiration during the path of this work. His continuous interest was a constant source of motivation for me throughout the work.

I would like to extend my special thanks to all my good friends for their kind help and cooperation in various ways during the course of this work.

# Table of Content

Acknowledgment .....	i
List of figures .....	iv
List of Tables .....	v
Abstract .....	vi
Chapter 1 .....	1
Introduction .....	1
1.1 Background .....	1
1.2 Objective of the work .....	3
1.3 Organization of the Thesis .....	4
Chapter 2 .....	5
Literature Review .....	5
Chapter 3 .....	13
Geometry and Finite Element Formulation of Helical Gear .....	13
3.1 Geometry of Helical Gear .....	13
3.2 Finite Element Formulation .....	18
3.3 Three-Dimensional Solid Element Formulation .....	18
3.4 Strain - Displacement Matrix [B] .....	19
3.5 Element Stiffness Matrix .....	22
3.6 Evaluation of Stresses .....	23
3.7 Stresses at the Center of the Element .....	23
3.8 Stresses on the Faces of the Element .....	23
Chapter 4.....	26
Solid Modeling and FEM Packages .....	26
4.1 Solid Modeling .....	26
4.2 Design of Gear by Solid Modeling .....	26
4.3 What is Pro/Engineer? .....	27
4.3.1 Feature-Based Nature of Pro/Engineer .....	27
4.3.2 Bi-Directional Associative Nature of Pro/Engineer .....	27
4.3.3 Parametric Nature of Pro/Engineer .....	28

4.4 Modeling Involute Gears in Pro/Engineer .....	28
4.5 General Procedures to Create an Involute Curve .....	29
4.6 FEM Package .....	31
Chapter 5 .....	32
Involute Gear Tooth Bending and Contact Stress Analysis .....	32
5.1 Introduction .....	32
5.2 Analytical Bending Stress Analysis.....	32
5.3 FEM Bending Stress Analysis.....	35
5.4 Comparison of Results using AGMA Bending Stress Formula.....	37
5.5 Contact Stress Analysis.....	38
5.6 Numerical Example of Contact Stresses between two Circular Cylinders.....	39
5.7 Results and Comparison of the Contact Stresses Analysis.....	41
5.8 Parametric Study.....	48
5.9 Results and Discussions .....	48
5.10 Effect of Face width.....	48
5.11 Effect of Helix angle .....	49
5.12 Combined effect of face width and helix angle.....	51
Chapter 6 .....	53
Conclusion and Future Work .....	53
6.1 Conclusion.....	53
6.2 Recommendation and Future work.....	54
References .....	55

## List of Figures

Figure 2.1 Illustration of line of action “A” on plane $\Pi$ .....	10
Figure 3.1 Angle of twist between ( $\theta_c$ ) any two faces.....	13
Figure 3.2 Angular position of point P in face 1.....	14
Figure 3.3 The representation of similar points $p(i, j)$ on subsequent faces with respect to the first face. ....	15
Figure 3.4 Total angle of twist.....	16
Figure 3.5 Over all geometry representation.....	17
Figure 3.6a Cartesian coordinate system .....	18
Figure 3.6b Local Coordinate system.....	18
Figure 4.1 Solid model of helical generated by Pro/Engineer.....	30
Figure 5.1 The cross section and the dimensions of gear tooth profile to determine the Lewis formula.....	33
Figure 5.2 Three-dimensional FEM model with 28 teeth.....	35
Figure 5.3 Von Mises stress of 28 number of teeth modeled gear.....	36
Figure 5.4 Ellipsoidal –prism pressure distribution.....	39
Figure 5.5 Two steel cylinders pressing against each other.....	41
Figure 5.6 Loading, boundary condition and meshing of half of the cylinders.....	42
Figure 5.7 The distribution of normal contact stress along the contact area.....	43
Figure 5.8 The distribution of maximum shear stress from ANSYS.....	46
Figure 5.9 The distribution of orthogonal shear stress from ANSYS.....	47
Figure 5.10 Graphical representation of Effect of face width on maximum bending stress.....	49
Figure 5.11 Graphical representation of Effect of helix angle on maximum bending stress.....	50
Figure 5.12 Graphical representation of the combined effect of face width and helix angle.....	52

## List of Tables

Table 4.1 Key geometrical parameters of helical gear used .....	30
Table 5.1 Maximum bending stresses (Von Mises) obtained from ANSYS .....	37
Table 5.2 Bending stress from AGMA formula .....	37
Table 5.3 Comparisons of maximum bending stresses .....	38
Table 5.4 Parameters of helical gear used .....	41
Table 5.5 Comparison of peak values of the equivalent stresses .....	45
Table 5.6 Effect of face width on maximum bending stress.....	48
Table5.7 Effect of helix angle on maximum bending stress.....	50
Table5.8 The combined effect of face width (b) and helix angle ( $\beta$ ).....	51

## **Abstract**

Gears are one of the most critical components in mechanical power transmission systems. The bending and surface strength of the gear tooth are considered to be one of the main contributors for the failure of the gear in a gear set. Thus, analysis of stresses has become popular as an area of research on gears to minimize or to reduce the failures and for optimal design of gears. This thesis investigates the characteristics of an involute helical gear system mainly focused on bending and contact stresses using analytical and finite element analysis.

To estimate the bending stress, three-dimensional solid models for different number of teeth are generated by Pro/Engineer that is a powerful and modern solid modeling software and the numerical solution is done by ANSYS, which is a finite element analysis package. The analytical investigation is based on Lewis stress formula.

This thesis also considers the study of contact stresses induced between two gears. Present method of calculating gear contact stress uses Hertz's equation. To determine the contact stresses between two mating gears the analysis is carried out on the equivalent contacting cylinders. The results obtained from ANSYS are presented and compared with theoretical values.

Face width and helix angle are important geometrical parameters in determining the state of stresses during the design of gears. Thus, in this work a parametric study is conducted by varying the face width and helix angle to study their effect on the bending stress of helical gear.

# Chapter 1

## Introduction

### 1.1 Background

Gearing is one of the most effective methods transmitting power and rotary motion from the source to its application with or without change of speed or direction. Gears will prevail as a critical machine element for transmitting power in future machines due to their high degree of reliability and compactness. The rapid development of heavy industries such as vehicle, shipbuilding and aircraft industries require advanced application of gear technology.

A gearbox consists of a set of gears, shafts and bearings that are mounted in an enclosed lubricated housing. They are available in a broad range of sizes, capacities and speed ratios. Their function is to convert the input provided by the prime mover into an output with lower speed and corresponding higher torque. In this thesis, analysis of the characteristics of helical gears in a gearbox is studied using finite element analysis.

The crucial requirement of effective power transmission in various machines, automobiles, elevators, generators, etc.... has created an increasing demand for more accurate analysis of the characteristics of gear systems. For instance in automobile industry highly reliable and lightweight gears are essential. Further more the best way to diminution of noise in engine requires the fabrication of silence gear system. Noise reduction in gear pairs is especially critical in the rapidly growing today's technology since the working environment is badly influenced by noise. The most successful way of gear noise reduction is attained by decreasing of vibration related with them. The reduction of noise by vibration control can be achieved through a research endeavor by an expert in the field.

Helical gears are currently being used increasingly as a power transmitting gear owing to their relatively smooth and silent operation, large load carrying capacity and higher operating speed. Designing highly loaded helical gears for power transmission systems that are good in strength and low level in noise necessitate suitable analysis methods that can easily be put into practice and also give useful information on contact and bending

stresses [3]. The finite element method is proficient to supply this information but the time required to generate proper model is a large amount. Therefore to reduce the modeling time a preprocessor method that build up the geometry required for finite element analysis may be used, such as Pro/Engineer. Pro/Engineer can generate three-dimensional models of gears. In Pro/Engineer the generated model geometry is saved as a file and then transferred to ANSYS for analysis.

The major cause of vibration and noise in a gear system is the transmission error between the meshing gears. By definition transmission error is the difference between the theoretical and the actual position between driving gear and the driven gear. It can be defined also as the amount by which the ratio at a given point in a revolution departs from the correct ratio. For this reason, with prior knowledge of the operating conditions of the gear set it is possible to design the gears with minimum vibration and noise.

Mostly transmission error is due to two major causes. The first cause is production incorrectness as well as mounting mistake and the second one is caused by elastic deflection at the time of loading. Transmission error is considered as one of the main contributor to noise and vibration in a gear system. This suggests that the gear noise is closely related to transmission error. If a pinion and a gear have ideal involutes profiles running with no loading they should theoretically run with zero transmission error. However, when these same gears transmit torque, the joint torsional mesh stiffness of each gear changes throughout the mesh cycle as the teeth deflect causing variations in angular rotation of the gear body. Even though the transmission error is relatively small these slight variations can cause noise at a frequency which matches a resonance of the shafts or the gear housing causes noise to be enhanced. This phenomenon has been actively studied in order to minimize the amount of transmission error in gears.

Gear analysis can be performed using analytical methods which required a number of assumptions and simplifications which aim at getting the maximum stress values only but gear analyses are multidisciplinary including calculations related to the tooth stresses and to failures like wear. In this thesis, an attempt will be made to analyze static contact and bending stresses to resist bending of helical gears, as both affect transmission error.

Due to the progress of computer technology many researchers tended to use numerical methods to develop theoretical models to calculate the effect of whatever is studied. Numerical methods are capable of providing more truthful solution since they require very less restrictive assumptions. However, the developed model and its solution method must be selected attentively to ensure that the results are more acceptable and its computational time is reasonable.

## **1.2 Objective of this work**

There have been plenty of research work investigations by so many researchers in gear systems that are discussed in the next chapter. Still there it remains to be developed an acceptable numerical approach, which is able to determine the variation in the geometry of gear contact and bending stresses. Helical gears have become a subject of research interest because the dynamic load, attention of the noise level during operation and the demand for lighter and smaller in size. In such type of gears there is a problem of failures at the root of the teeth because of the inadequate bending strength and surface pitting. This can be avoided or minimized by proper method analysis and modification of the different gear parameters. In view of this the main purpose of this thesis is by using numerical approach to develop theoretical model of helical gear in mesh and to determine the effect of gear tooth stresses. The main focusing areas of this paper is described as follow:

- ❖ Modeling the gear without losing its geometry in Pro/engineer software.
- ❖ Develop and determine models of contact elements, to analysis contact stresses using ANSYS and compare the result with Hertzian theory.
- ❖ Generate the profile of helical gear teeth model to calculate the effect of gear bending, using three-dimensional model and compare the results with Lewis theory.
- ❖ Perform parametric study to study the effect of face width and helix angle on the bending stress.

To accomplish these objectives an effort will be made in this work to develop suitable three-dimensional model and finite element analysis will be used to study the stresses.

### **1.3 Organization of the Thesis**

This thesis is organized from a total of six chapters. Chapter 1 gives detailed information about the general introduction, objectives to be achieved and organization of the thesis. Chapter 2 is literature review, which are done by various researchers. Chapter 3 describes analytical method of developing helical gear geometry, it also illustrate the finite element formulation of helical gear using eight-nodded solid element with isoparametric formulation. Chapter 4 gives concise information on solid modeling, about commercial software such as Pro/Engineer and ANSYS and general procedures for modeling involute gear. Chapter 5 presents detailed information about the analysis of bending ,contact stresses and parametric study. It shows also the comparison of results. Chapter 6 provides the conclusion obtained from this work and suggests future work in this area.

## Chapter 2

### LITERATURE REVIEW

There are great deal of researches and number literatures on gear analysis that has been published. Generally their major concerns are on the analysis of gear stresses, transmission errors, dynamic loads, noise, and failure of gear tooth, which are very useful for optimal design of gear set. They have used various approaches and means to attain their main intention. The first systematic studies in gear dynamics started in the 1920s by A.A Ross and E.Buckingham [1]. The basic concern in their studies was the prediction of tooth dynamic loads for designing gears at higher speeds.

This research attempts to review literatures, which are relevance to analysis gear of stresses.

Isay and Fong [2] applied the tooth contact analysis technique (TCA) and finite element method (FEM) to gear contact and stress analysis. In their study, a mathematical model for pinion and gear involutes teeth is assumed. The geometry of the gears are described by parameters of manufacturing. Computer simulations of the conditions of gear meshing including the axes misalignment and center distance variation are performed. Their paper showed that the locations of bearing contact and contact pattern of mating tooth surfaces are determined by TCA techniques. The results of the TCA provide the location and the direction of applied loads for the computer aided FEM stress analysis,by applying the given mathematical model and TCA techniques. A three-dimensional stress analysis for this type of gearing was investigated by Von-Mises stress contour distribution.

Vljayaragan and Ganesan [4] presented a static analysis of composite helical gears system using three dimensional finite element methods to study the displacements and stresses at various points on a helical gear tooth. The validity of their results of the FEM was tested by the root stress for C-45 steel material gear and comparing the result with obtained from conventional gear design equation. The paper presented also the evaluation of the performance of composite helical gears by companion of with that of the

conventional carbon steel gear. It is observed from the result that composite materials can be used safely for power transmission helical gears but the face width has to be suitably increased.

Huston et al [28] discussed a new approach to modeling gear tooth surfaces. A computer graphics solid modeling procedure is used to simulate the tooth fabrication processes. This procedure is based on the principle of differential geometry that pertains to envelopes of curves and surfaces. The procedure is illustrated with the modeling of spur, helical, bevel, spiral bevel and hypoid gear teeth. Applications in design and Manufacturing are discussed. Extensions to nonstandard tooth forms, to cams, and to rolling element bearings are proposed.

In 1992, Rao and Muthuveerappan [6] explained about the geometry of helical gears by simple mathematical equations, the load distribution for various positions of the contact line and the stress analysis of helical gears using the three dimensional finite element methods. A computer program has been developed for the stress analysis of the gear. Root stresses are evaluated for different positions of the contact line when it moves from the root to the tip. To check the validity of the developed program, the changes in the trend of the maximum root stress values at various places of the tooth along the face width were compared with the experimental results. A parametric study was made by varying the face width and the helix angle to study their effect on the root stresses of helical gears. Based on their investigation the effect of helix angle and face width on the root stresses of helical gears was clarified for different positions of the contact line.

In a paper by Litvin and Chen [8], load share and finite element stress analysis for double circular arc helical gears is presented. The authors analyzed the tooth surface contact and stresses their approach was based on the application of computerized simulation of meshing and contact loaded gear drives and the finite element method. They investigated the conditions of load share under a load and determined the real contact ratio for aligned and misaligned gear drives, respectively. Elastic deformation of teeth and the stress

analysis of the double circular are helical gears are accomplished by using finite element method. The finite element models for the pinion and gear are constructed respectively. The stress analyses for aligned and misaligned have been compared with those obtained by other approaches.

In 1998, a method namely the normal stiffness matrix along contact line (NSMCL) for analyzing cylindrical gears was proposed by Jianfeng et al [10]. The method established three dimensional finite element models for spur and helical gears; external and internal hobbling and slotting, different parameters and materials can be analyzed using these models. Results such as load distribution along the contact lines, deformations and stiffness at any position, and contact stresses are presented. The calculated results show that the trend of gear tooth deformation coincides with the tested ones using the dynamic speckle photography method.

In 1999, Jianfens et al. [13] also presented finite element analysis of instantaneous mesh stiffness of cylindrical gears. Based on the analysis of the profile formulation principle of internal and external mesh gears of hobbling and slotting three dimensional highly accurate solid models of gear teeth have been established, which take the accurate fillet curve and non-simplification tooth profile into consideration. The contact range and the whole finite element model can be automatically adjusted with the change of meshing process. Instantaneous mesh stiffness of spur and helical gears with and without flexible gear body, have been obtained.

In the same year, a new approach was introduced by Zhang et al [16] to analyze the loading and stress distribution of spur and helical gears accounting for the varying meshing stiffness, geometric modification and elastic deflection of engaged gears. Combining a discretized gear model with finite element analysis it has both good computational accuracy and efficiency.

Zhang and Fang [19] presented an approach for the analysis of teeth contact and load distribution of helical gears with crossed axis. The approach was based on a tooth contact model that accommodates the influence of tooth profile modifications, gear manufacturing errors and tooth surface deformation on gear mesh quality. In the approach the tooth contact load is assumed to be distributed along the tooth surface line that coincides with the relative principal direction of the contacting tooth surface. As compared with existing tooth contact analysis model that assumes rigidity for the contacting surfaces the model in this paper provides a more realistic analysis on gear transmission errors, contact patterns and the distribution of contact load. As a numerical example, the contact of a pair of helical gears with a small crossing angle is analyzed by computer program that implements the approach it is found from the analysis that helical gears with small crossing angle have meshing characteristics and load distribution similar to those of parallel axis gears.

Chen and Tsay [21] investigate the contact and the bending stresses of helical gear set with localized bearing contact by means of finite element analysis (FEA). The proposed helical gear set comprises an involute pinion and double crowned gear. Mathematical models of the complete teeth geometry of the pinion and the gear have been derived based on the theory of gearing. Accordingly, a mesh generation program was also developed for finite element stress analysis. The gear stress distribution is investigated using the commercial FEA package, ABAQUS standard. Furthermore, several examples are presented to demonstrate the influences of the gear's design parameters and the contact positions on the stress distribution.

The paper, which covered design, generation tooth contact analysis and stress analysis of a new type of Novikov-wildhaber helical gear drive was presented by Litvin et al [23]. In the paper, computer programs for computerized design tooth contact analysis, and automatic development of finite element models of the given gear drives have been developed. Stress analysis and investigation of bearing contact have performed by using finite element analysis. The developed theory is illustrated with numerical examples.

The computerized design, methods for generation, simulation of meshing, and enhanced stress analysis of modified involute helical gears was considered by Litvin et al [35]. The approaches proposed for modification of conventional involute helical gears were based on conjugation of double-crowned pinion with a conventional helical involute gear. Double-crowning of the pinion means deviation of cross-profile from an involute one and deviation of longitudinal direction from a helicoids surface. Using the method developed, the pinion-gear tooth surface was in point-contact, the bearing contact was localized and oriented longitudinally, and edge contact was avoided. Also, the influence of errors of alignment on the shift of bearing contact, vibration, and noise were reduced substantially. The theory developed was illustrated with numerical examples that confirm the advantages of the gear drives of the modified geometry in comparison with conventional helical involute gears.

Park and Yoo [31] presented study of deformation overlap in the design of spur and helical gear pair. Deformation overlap that is numerically calculated quantity through displacement analysis at the initial contact is defined as the piled region of a contact tooth pair due to the elastic deformation. It is suggested for an effective indicator to represent the whole deformation of meshing gear pair. The contact theory and finite element method are used to compute the contact force and tooth deflection. The contact forces between teeth are determined from the transmitted torque, then the deformation overlap is calculated with the contact forces as boundary conditions. For spur gear pair, the computed deformation overlap is used for the basis of the teeth tip relief, analysis of deformation characteristics for a profile shifted gear pair, and the selection of profile shift coefficient considering teeth deflection. Deformation overlap is also extended to three-dimensional problems and implemented to helical gear pair.

A paper on generalized concept of meshing and contact of involute crossed helical gears and its application was presented by Fuentes et al [32]. In their paper, a general approach for generation and design of standard and non-standard involute crossed helical gears is proposed. The conjugation of gear tooth surfaces is based on application of two generating rack-cutters with a common normal section. The investigation of the geometry is based on a new approach for presentation of the line of action “A” (the line of point’s contact of tooth surfaces) line “A” is represented in a plane  $\Pi$  that is tangent to the pinion base cylinder and position of “A” is determined analytically. Edge contact of tooth surfaces is avoided by limitation of shift of line of action caused by errors  $\Delta\gamma$  and  $\Delta E$  of the crossing angle and the shortest distance, respectively. Simulation of meshing and contact is computerized by developed computer program. Enhanced stress analysis approach is also proposed. The developed theory is illustrated with numerical example.

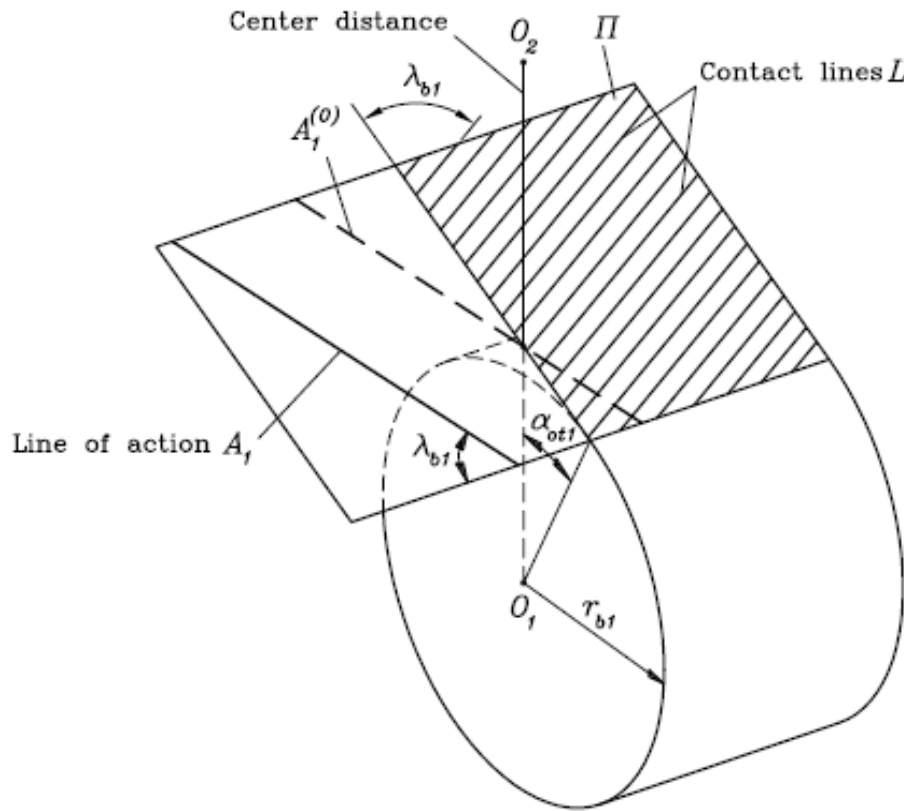


Figure 2.1 Illustration of line of action “A” on plane  $\Pi$ .

Hedlund and Lehtovaara [33] presented a study focuses on the modeling of helical gear contact with tooth deflection. Their paper introduced a mathematical model for helical gear contact analysis. Helical gear surface profiles are constructed from gear tooth geometry by simulation the hobbing process. The three-dimensional finite element model for the calculation of tooth deflection including tooth bending, shearing and tooth foundation flexibility. The model combines contact analysis with structural analysis to avoid large meshes. Tooth foundation flexibility was found to have an essential role in contact load sharing between the meshing teeth where as contact flexibility plays only a minor role. The capability of different local contact calculation methods was also studied.

A mathematical model was developed to calculate the fatigue life of pinion, gear or gear set by Coy and Zaretsky [34]. They derived also an equation for the dynamic capacity of a gear set. Dynamic capacity is the transmitted tangential load that gives a ninety percent probability of survival of the gear set for one million pinion revolutions. The equations, when simplified by setting the helix angle to zero, reduce to the equations to spur gears. A sample calculation is given which illustrates the use of new fatigue model.

Wagaj and Kahraman [24] considered a non-linear finite element contact mechanics model of a parallel axis gear to study the impact of intentional tooth flank modifications on the static motion transmission error of the gear fair. In their paper, an experimental study is performed for the validation of the model predications. The validated model is then employed to investigate the impact of both two - dimensional (2D) and three – dimensional (3D) tooth flank modifications on the transmission error excitation. In case of 2D modifications, a parameter set that includes the magnitude, extent and (type linear or quadratic) of involute tip modifications and lead crown is considered. For 3D modifications, parameters defining both “bias-in” and “bias-out” type of modifications are included. The combined influence of modification parameters and load transmitted on the resultant unit transmission error excitation is quantified.

A basis for solid modeling of gear teeth with application in design and manufacture was investigated by Huston et al [28]. They discussed a new approach to modeling of gear tooth surfaces. A computer graphics solid modeling is used to simulate the tooth fabrication processes. This procedure is based on the principles of differential geometry that pertain to envelopes of curves and surfaces. The procedure is illustrated with modeling of spur, helical, bevel, spiral bevel and hypoid gear teeth. Applications in design and manufacturing are discussed. Extensions to nonstandard tooth forms, to cams and to rolling element bearings are proposed.

Litvin and Fuentes studied the geometry, generation by a shaper and a worm avoidance of singularities and stress analysis of face gear drive with helical involute pinion [35]. In their study, a new type of face gear drive with conjugated face gear and generation of face gears by a shaper free of undercutting and pointing have been investigated. A new method for grinding or cutting of face gears by worm of special shape has been developed. A computerized design procedure has been developed to avoid undercutting and pointing by a shaper or by generating worm. Also, a method to determine the limitation of the helix angle magnitude was developed. The method provides a localization of the bearing contact to reduce the shift of bearing contact by misalignment. The analytical method provides simulation of the meshing and contact of misaligned gear drives. An automatic mesh generation method has been developed and used to conduct a three-dimensional contact stress analysis of several teeth. The theory developed is illustrated with several examples.

Vera and Ivan [26] used the numerical method for modeling the contact of tooth flanks to analyzed and determine the shape of the function which defines the change of contact stresses on tooth flanks along the path of contact for a tooth pair. The paper provides the detailed description of model development procedure. The results provided for the stress state of tooth flanks are also presented and discussed. The comparison of analytically and numerically obtained curves of change in the stress state on meshed tooth flanks, confirmed the accrual of the developed model.

## Chapter 3

### GEOMETRY AND FINITE ELEMENT FORMULATION OF HELICAL GEAR

#### 3.1 Geometry of Helical Gear

Like other gears, helical gears are employed to transmit motion between parallel, non-parallel and non-intersecting shafts. In the former case the gears are called parallel helical gears while in the later case they are termed as crossed helical gears. The analytical development of helical gear tooth geometry is complicated in nature due to the curved shape of the tooth along the face width. An involute helical gear is analogous to a set of stepped gears, which consists of identical large number of small face-width spur gears. Each of the spur gears being rotated with respect to the previous one so as to form the helix.

The profile of the front face of the gear tooth with the transverse module as spur gear is computed and obtained by using AutoCAD. Then to get the coordinates of the corresponding points on the subsequent faces while being rotated from the first face at any plane along the face width were obtained by the following procedure [5].

The helix angle  $\beta_c$  shown in Figure 3.1 at any radius  $r_c$  can be defined as

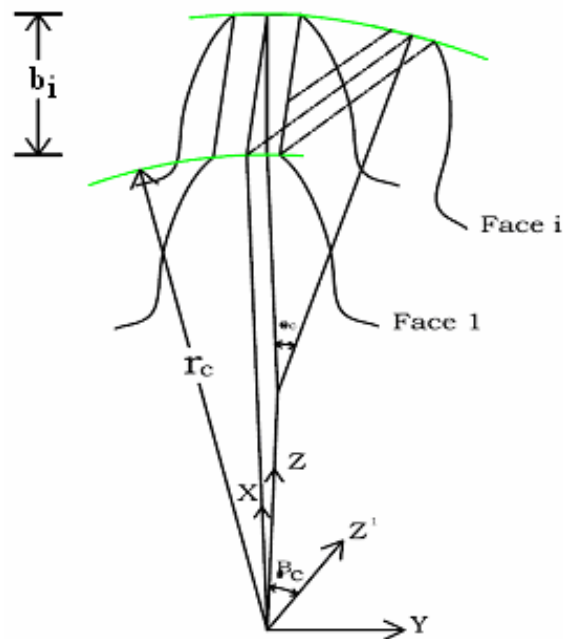


Figure 3.1 Angle of twist between ( $\theta_c$ ) any two faces

$$\tan \beta_c = \left[ \frac{(\tan \beta \times r_c)}{r} \right] \quad , \text{ where } r \text{ is pitch circle radius.}$$

and in terms of angle of twist, it can be defined as

$$\tan \beta_c = \left[ \frac{(\theta_c \times r_c)}{b_i} \right] \quad \text{where } b_i = \text{face width}$$

$$\text{or } \theta_c = \frac{(b_i \times \tan \beta_c)}{r_c} \quad \dots\dots\dots(1)$$

Considering a point  $(p_{ij})$  from Figure 3.2 on the boundary of the first face of the gear tooth generated, whose coordinate is  $(x_j, y_j)$  where  $(0, 0)$  is assumed as a gear centre in the first face (where  $i = 1$  for the first face and  $j = 1$ , total number of nodal points in a face under consideration). For any point on face 1, the angle  $\theta_{ij}$  is defined as

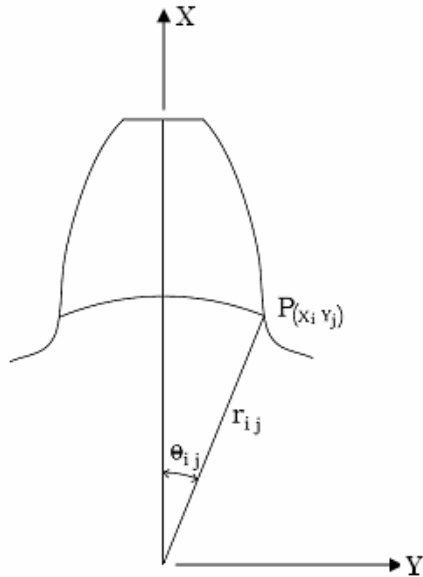


Figure 3.2 Angular position of point P in face 1

$$\tan \theta_{1j} = \frac{y_{1j}}{x_{1j}}$$

$$\theta_{1j} = \tan^{-1} \left( \frac{y_{1j}}{x_{1j}} \right)$$

$$\text{Therefore, } r_{1j}^2 = (x_{1j}^2 + y_{1j}^2)$$

For any other corresponding point lying on any one of the subsequent faces which is shown in Figure 3.3, the angle of twist  $\theta_{ij}$  with respect to the first face due to the helix angle as described by equation (1) is modified to give

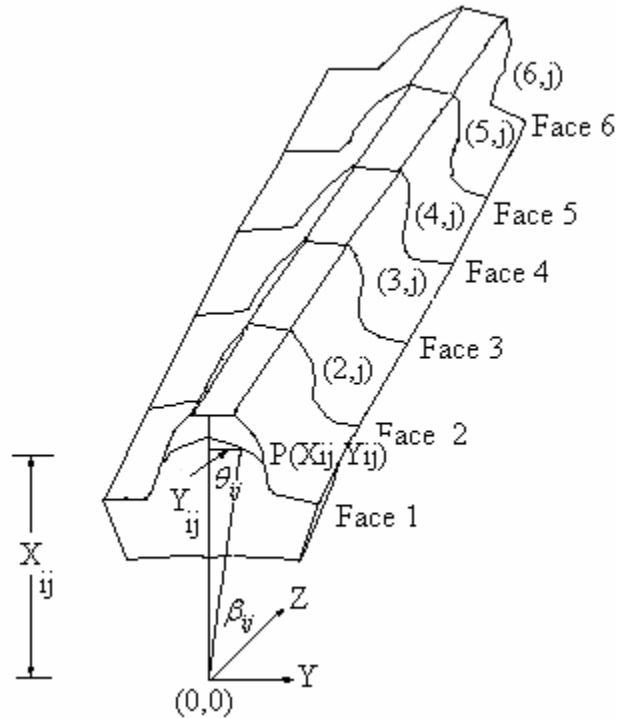


Figure 3.3 the representation of similar points  $p(i, j)$  on subsequent faces with respect to the first face.

$$\tan \beta_{ij} = \left( \frac{r_{ij} \times \theta_{ij}}{b_i} \right) \dots\dots\dots (2)$$

Where  $i = 1, 2, \dots, n$  (number of faces) and  $j = 1, 2, \dots, m$  (number of nodes in each faces) that is

$$\theta_{ij} = \left( \frac{b_i \times \tan \beta_{ij}}{r_{ij}} \right)$$

Therefore the total angle of twist of the a corresponding point in any face ( $i$ ) with respect to the first face which is shown in Figure 3.4 is given as

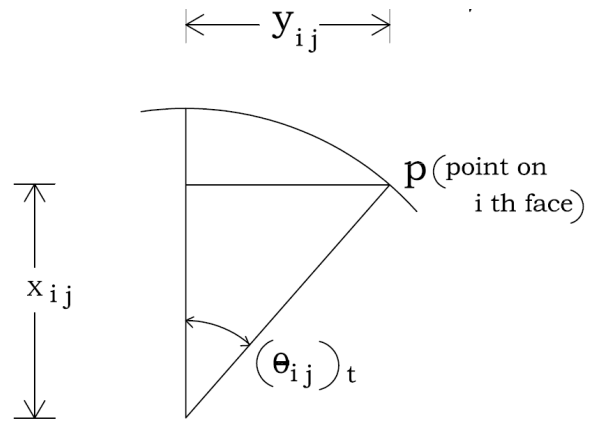


Figure 3.4 Total angle of twist

$$(\theta_{ij})_t = \theta_{1j} + \theta_{ij}$$

The overall representation of geometry of helical gear tooth is shown in Figure 3.5. the numbers 1, 2, 3 and 4 in the figure indicates the corresponding angles  $\theta_c, \theta_{1j}$  and  $(\theta_{ij})_t$ .

The coordinates of any point on any subsequent faces of the gear tooth can now be defined as

$$x_{ij} = r_{ij} \times \cos(\theta_{ij})_t$$

$$y_{ij} = r_{ij} \times \sin(\theta_{ij})_t$$

$$z_{ij} = b_1$$

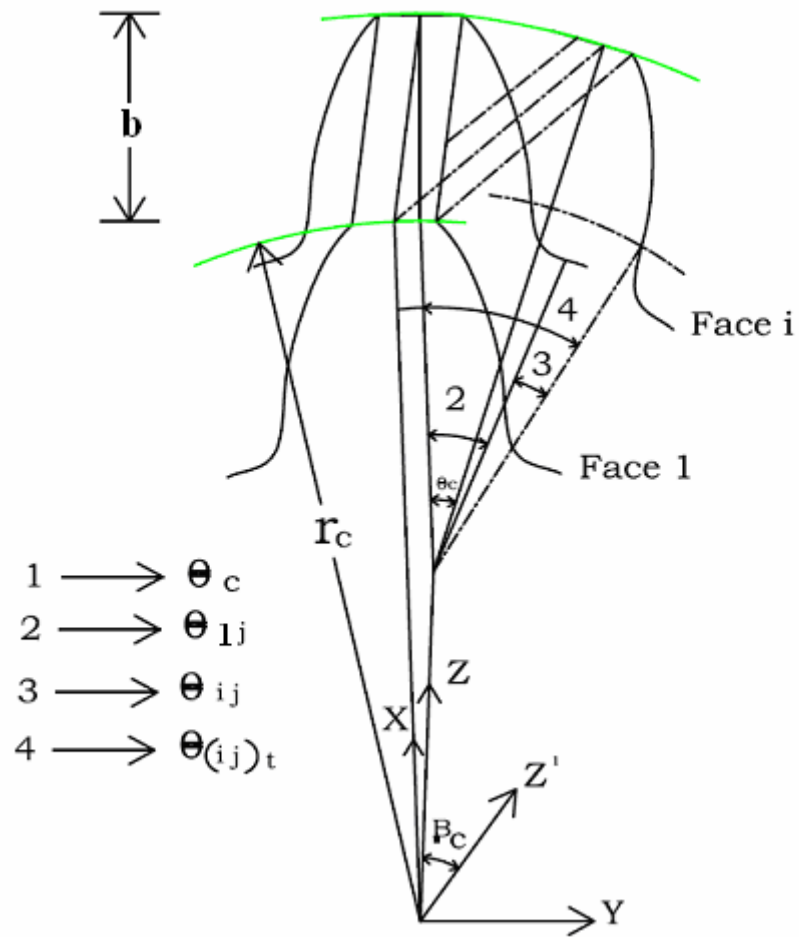


Figure 3.5 over all geometry representation

After finding out the coordinates of all the nodal points the helical gear tooth can be generated.

### 3.2 Finite Element Formulation

For three-dimensional stress analysis solid elements are useful for the solution of problems. These solid elements are broadly grouped under tetrahedral, triangular and hexahedral family elements.

In this thesis, the three-dimensional eight noded solid element is chosen from hexahedral family for the element representation that uses for three dimensional analysis based isoparametric formulation. This is because for the analysis of some components of complex shapes involving curved boundaries or surfaces, like helical gears simple triangular or rectangular elements are no longer sufficient.

The concept of isoparametric element is based on the transformation of parent element in local or natural coordinate to system to an arbitrary shape in Cartesian coordinate system [17].

### 3.3 Three-Dimensional Solid Element Formulation

The three dimensional eight noded solid element shown in Figure 3.6 has eight nodes located at the corners and three translational degree of freedom at each node. The shape function defining the geometry and the variation of displacement is given by

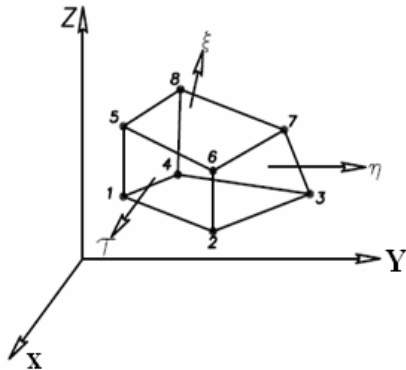


Figure 3.6a Cartesian coordinate system

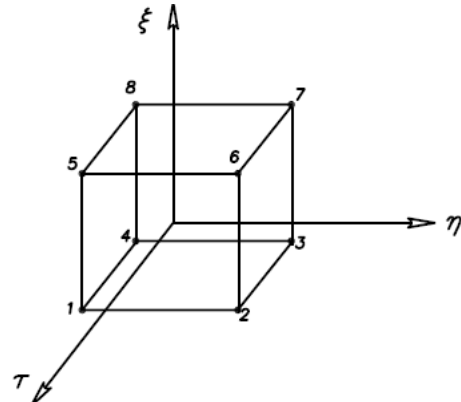


Figure 3.6b Local Coordinate system

$$N = \frac{1}{8}(1 + \tau\tau_i)(1 + \eta\eta_i)(1 + \xi\xi_i) \quad i = 1,2,\dots,8 \quad [17] \quad \dots\dots\dots(3.1)$$

Where  $\tau, \eta, \xi$  are natural coordinates and  $\tau_i, \eta_i$  and  $\xi_i$  are the values of the coordinates for node  $i$ .

Thus, the geometry of the element can be represented by a matrix as,

$$\begin{Bmatrix} x \\ y \\ z \end{Bmatrix} = \sum_{i=1}^8 N_i(\tau, \eta, \xi) \begin{Bmatrix} x_i \\ y_i \\ z_i \end{Bmatrix} \dots\dots\dots (3.2)$$

Where  $x_i, y_i, \text{and } z_i$  are the global coordinates of node  $i$ .

The variation of displacement inside the element is expressed using the same functions as,

$$\begin{Bmatrix} u \\ v \\ w \end{Bmatrix} = \sum_{i=1}^8 N_i(\tau, \eta, \xi) \begin{Bmatrix} u_i \\ v_i \\ w_i \end{Bmatrix} \dots\dots\dots (3.3)$$

Where  $u_i, v_i, \text{and } w_i$  are nodal displacements of node  $i$  in the Cartesian coordinate system.

**3.4 Strain - Displacement Matrix [B]**

The finite element formulation is done in terms of natural coordinates so it is necessary to drive the relation between the derivatives of functions in the natural coordinates and the derivates in the Cartesian coordinates. This is achieved by evaluating by using the Jacobian as follow: -

$$\begin{Bmatrix} \frac{\partial}{\partial \tau} \\ \frac{\partial}{\partial \eta} \\ \frac{\partial}{\partial \xi} \end{Bmatrix} = [J] \begin{Bmatrix} \frac{\partial}{\partial x} \\ \frac{\partial}{\partial y} \\ \frac{\partial}{\partial z} \end{Bmatrix} \dots\dots\dots (3.4)$$

Where the Jacobian [J] is given by,

$$[J] = \begin{bmatrix} \frac{\partial x}{\partial \tau} & \frac{\partial y}{\partial \tau} & \frac{\partial z}{\partial \tau} \\ \frac{\partial x}{\partial \eta} & \frac{\partial y}{\partial \eta} & \frac{\partial z}{\partial \eta} \\ \frac{\partial x}{\partial \xi} & \frac{\partial y}{\partial \xi} & \frac{\partial z}{\partial \xi} \end{bmatrix} \dots\dots\dots (3.5)$$

Inserting equation (3.2) in equation (3.5), it gives

$$[J] = \begin{bmatrix} x_i \frac{\partial N_i}{\partial \tau} & y_i \frac{\partial N_i}{\partial \tau} & z_i \frac{\partial N_i}{\partial \tau} \\ x_i \frac{\partial N_i}{\partial \eta} & y_i \frac{\partial N_i}{\partial \eta} & z_i \frac{\partial N_i}{\partial \eta} \\ x \frac{\partial N_i}{\partial \xi} & y_i \frac{\partial N_i}{\partial \xi} & z_i \frac{\partial N_i}{\partial \xi} \end{bmatrix} \dots\dots\dots (3.6)$$

The inverse of the above matrix can be symbolically written as,

$$[J]^{-1} = \begin{bmatrix} J^* & J^* & J^* \\ J^* & J^* & J^* \\ J^* & J^* & J^* \end{bmatrix} \dots\dots\dots (3.7)$$

The strain-displacement relation can be written as,

$$\{\varepsilon\} = [B][d] \dots\dots\dots (3.8)$$

Where  $\{d\}^T = [u_1 v_1 w_1 \dots \dots \dots u_8 v_8 w_8]$

This equation can be written as,

$$\{\varepsilon\} = \sum_{i=1}^8 [B_i] \{d_i\} \dots\dots\dots (3.9)$$

The strain components are given by

$$\{\varepsilon\} = \begin{Bmatrix} \frac{\partial u}{\partial x} \\ \frac{\partial v}{\partial y} \\ \frac{\partial w}{\partial z} \\ \frac{\partial u}{\partial y} + \frac{\partial v}{\partial x} \\ \frac{\partial v}{\partial z} + \frac{\partial w}{\partial y} \\ \frac{\partial u}{\partial z} + \frac{\partial w}{\partial x} \end{Bmatrix} \dots\dots\dots (3.10)$$

To get the derivatives of the displacement in global coordinates first, it is necessary to get the derivatives of the displacement in natural coordinates. Therefore, differentiating equation (3.3) with respect to  $\tau, \eta, \xi$  gives,

$$\begin{Bmatrix} \frac{\partial u}{\partial \tau} & \frac{\partial v}{\partial \tau} & \frac{\partial w}{\partial \tau} \\ \frac{\partial u}{\partial \eta} & \frac{\partial v}{\partial \eta} & \frac{\partial w}{\partial \eta} \\ \frac{\partial u}{\partial \xi} & \frac{\partial v}{\partial \xi} & \frac{\partial w}{\partial \xi} \end{Bmatrix} = \sum_{i=1}^8 \begin{Bmatrix} \frac{\partial N}{\partial \tau} u_i & \frac{\partial N}{\partial \tau} v_i & \frac{\partial N}{\partial \tau} w_i \\ \frac{\partial N}{\partial \eta} u_i & \frac{\partial N}{\partial \eta} v_i & \frac{\partial N}{\partial \eta} w_i \\ \frac{\partial N}{\partial \xi} u_i & \frac{\partial N}{\partial \xi} v_i & \frac{\partial N}{\partial \xi} w_i \end{Bmatrix} \dots\dots\dots (3.11)$$

Now by using the Jacobian inverse that expressed in equation (3.7) the derivatives of the displacement in global coordinates can be written as,

$$\begin{Bmatrix} \frac{\partial u}{\partial x} & \frac{\partial v}{\partial x} & \frac{\partial w}{\partial x} \\ \frac{\partial u}{\partial y} & \frac{\partial v}{\partial y} & \frac{\partial w}{\partial y} \\ \frac{\partial u}{\partial z} & \frac{\partial v}{\partial z} & \frac{\partial w}{\partial z} \end{Bmatrix} = [J]^{-1} \begin{Bmatrix} \frac{\partial u}{\partial \tau} & \frac{\partial v}{\partial \tau} & \frac{\partial w}{\partial \tau} \\ \frac{\partial u}{\partial \eta} & \frac{\partial v}{\partial \eta} & \frac{\partial w}{\partial \eta} \\ \frac{\partial u}{\partial \xi} & \frac{\partial v}{\partial \xi} & \frac{\partial w}{\partial \xi} \end{Bmatrix} \dots\dots\dots (3.12)$$

Expanding the above equation and substituting for  $u, v, w$  from equation (3.3) in the above equation it is possible to write the derivatives of displacement with respect to the Cartesian system and by using this derivatives the values of the matrices of  $[B_i]$  can be written as,

$$[B_i] = \begin{bmatrix} \frac{\partial N_i}{\partial x} & 0 & 0 \\ 0 & \frac{\partial N_i}{\partial y} & 0 \\ 0 & 0 & \frac{\partial N_i}{\partial z} \\ \frac{\partial N_i}{\partial y} & \frac{\partial N_i}{\partial y} & 0 \\ 0 & \frac{\partial N_i}{\partial y} & \frac{\partial N_i}{\partial z} \\ \frac{\partial N_i}{\partial z} & 0 & \frac{\partial N_i}{\partial x} \end{bmatrix} \dots\dots\dots (3.13)$$

Hence, the  $[B]$  matrix for equation (3.8) can be written as,

$$[B] = [[B_1][B_2][B_3][B_4][B_5][B_6][B_7][B_8]]$$

Where  $[B_1] \dots\dots\dots [B_8]$  are sub matrices with size  $6 \times 3$ .

### 3.5 Element Stiffness Matrix

The constitutive matrix  $[C]$  for isotropic three-dimensional stress analysis is given by [18],

$$[C] = \frac{E}{(1+\nu)(1-2\nu)} \begin{bmatrix} 1-\nu & \nu & \nu & 0 & 0 & 0 \\ \nu & 1-\nu & \nu & 0 & 0 & 0 \\ \nu & \nu & 1-\nu & 0 & 0 & 0 \\ 0 & 0 & 0 & \frac{1-2\nu}{2} & 0 & 0 \\ 0 & 0 & 0 & 0 & \frac{1-2\nu}{2} & 0 \\ 0 & 0 & 0 & 0 & 0 & \frac{1-2\nu}{2} \end{bmatrix} \dots\dots\dots (3.14)$$

Therefore, the element stiffness matrix is obtained as,

$$[K] = \int_{-1}^{+1} \int_{-1}^{+1} \int_{-1}^{+1} [B]^T [C] [B] J |d\tau d\eta d\xi \dots\dots\dots (3.15)$$

The element stiffness matrix is evaluated numerically using the Gaussian quadrature weighted functions.

### 3.6 Evaluation of Stresses

The stresses corresponding to the strains are calculated at the centre of the element and at the centers of the element faces. The stresses at the centre of the element are expressed in the global axes and the stresses on the faces in the local axes direction.

#### 3.7 Stresses at the Center of the element

The stress - displacement matrix is given by,

$$[CB] = [C][B] \dots\dots\dots (3.16)$$

Where  $[C]$  is the constitutive matrix given in equation (3.14) then the stress components at the centroid of the element is expressed as,

$$[\sigma] = [CB]\{d_a\} \dots\dots\dots (3.17)$$

Where,

$$[\sigma] = [\sigma_x \sigma_y \sigma_z \sigma_{xy} \sigma_{yz} \sigma_{xz}] \dots\dots\dots (3.18)$$

$$\{d_a\} = [u_1 v_1 w_1 \dots\dots\dots u_8 v_8 w_8] \dots\dots\dots (3.18)$$

#### 3.8 Stresses on the Faces of the Element

The strain vector with respect to the local axes is given by,

$$\{\varepsilon'\} = \begin{Bmatrix} \varepsilon'_x \\ \varepsilon'_y \\ \varepsilon'_z \\ \varepsilon'_{xy} \\ \varepsilon'_{yz} \\ \varepsilon'_{zx} \end{Bmatrix} = \begin{Bmatrix} \frac{\partial u'}{\partial x'} \\ \frac{\partial v'}{\partial y'} \\ \frac{\partial w'}{\partial z'} \\ \frac{\partial u'}{\partial y'} + \frac{\partial v'}{\partial x'} \\ \frac{\partial v'}{\partial z'} + \frac{\partial w'}{\partial y'} \\ \frac{\partial u'}{\partial z'} + \frac{\partial w'}{\partial x'} \end{Bmatrix} \dots\dots\dots (3.18)$$

Where,  $u'$ ,  $v'$  and  $w'$  are the displacement components along the local axes.

The strain components along the local axes can be obtained by using the relation,

$$\begin{bmatrix} \frac{\partial u'}{\partial x'} & \frac{\partial v'}{\partial x'} & \frac{\partial w'}{\partial x'} \\ \frac{\partial u'}{\partial y'} & \frac{\partial v'}{\partial y'} & \frac{\partial w'}{\partial y'} \\ \frac{\partial u'}{\partial z'} & \frac{\partial v'}{\partial z'} & \frac{\partial w'}{\partial z'} \end{bmatrix} = [D]^T \begin{bmatrix} \frac{\partial u}{\partial x} & \frac{\partial v}{\partial x} & \frac{\partial w}{\partial x} \\ \frac{\partial u}{\partial y} & \frac{\partial v}{\partial y} & \frac{\partial w}{\partial y} \\ \frac{\partial u}{\partial z} & \frac{\partial v}{\partial z} & \frac{\partial w}{\partial z} \end{bmatrix} [D] \quad \dots\dots\dots (3.19)$$

Where,

$[D]$  Is the direction cosine of the new axes  $x'$ ,  $y'$  and  $z'$  which is given by,

$$[D] = \begin{bmatrix} l_1 & l_2 & l_3 \\ m_1 & m_2 & m_3 \\ n_1 & n_2 & n_3 \end{bmatrix} \quad \dots\dots\dots (3.20)$$

Inserting the value of  $[D]$  into equation (3.19), evaluating and rearranging it give,

$$[\varepsilon'] = [T_\varepsilon] \{\varepsilon\} \quad \dots\dots\dots (3.21)$$

When  $[T_\varepsilon]$  the strain transformation matrix which is given,

$$[T_\varepsilon] = \begin{bmatrix} l_1^2 & m_1^2 & n_1^2 & l_1 m_1 & m_1 n_1 & n_1 l_1 \\ l_2^2 & m_2^2 & n_2^2 & l_2 m_2 & m_2 n_2 & n_2 l_2 \\ 2l_1 l_2 & 2m_1 m_2 & 2n_1 n_2 & l_1 m_2 + l_2 m_1 & m_1 n_2 + m_2 n_1 & n_1 l_2 + n_2 l_1 \\ 2l_2 l_3 & 2m_2 m_3 & 2n_2 n_3 & l_3 m_2 + l_2 m_3 & m_3 n_2 + m_2 n_3 & n_3 l_2 + n_2 l_3 \\ 2l_3 l_1 & 2m_3 m_1 & 2n_3 n_1 & l_3 m_1 + l_1 m_3 & m_3 n_1 + m_1 n_3 & n_3 l_1 + n_1 l_3 \end{bmatrix} \quad \dots\dots\dots (3.22)$$

From equation (3.8),

$$[\varepsilon] = [B] [d_a] \quad \dots\dots\dots (3.22)$$

Where  $[B]$  is the strain-displacement matrix, hence

$$[\varepsilon'] = [T_\varepsilon] [B] \{d_a\} \quad \dots\dots\dots (3.23)$$

That is,

$$\{\varepsilon'\} = [B'] [d_a] \quad \dots\dots\dots (3.24)$$

Where,

$$[B'] = [T_\varepsilon][B] \dots\dots\dots (3.25)$$

Then, the stresses on the faces are given by,

$$[\sigma'] = [CB'][d_a] \dots\dots\dots (3.26)$$

Where,

$[\sigma']$  is the stress vector on the local axes.

## Chapter 4

### Solid Modeling and FEM Packages

#### 4.1 Solid Modeling

Solid Modeling is geometrical representation of a real object without losing information the real object would have. It has volume and therefore, if some one provides a value for density of the material, it will have mass and inertia. Unlike the surface model, if one makes a hole or cut in a solid model, a new surface is automatically created and the model recognizes which side of the surface is solid material. The most useful thing about solid modeling is that it is impossible to create a computer model that is ambiguous or physically non-realizable [25].

#### 4.2 Design of Gear by Solid Modeling

The available gear design soft wares are mathematical in nature for the proper modeling of the involute curve and the tooth profile generated from the curve. Dedicated gear design programs perform the calculations, which are necessary to create the true profile of the gear tooth, but this is a tedious and time-consuming operation.

However, CAD/CAM applications can do this in seconds to generate a correct involute tooth profile quickly and easily due to their graphical nature. They are graphical modeling tools and there are a finite number of calculations they can perform and a finite number of points they plot along the involute curve.

CAD systems approximate shapes such as involute tooth profile by defining points along a curve and then simply connecting those points with a straight lines. The more points you can plot, the smaller the lines are used to draw the curve. While they can plot many of points along the curve, coming close to the involute profile, there is always an error due to the need for the software to approximate using points and lines.

Dedicated gear design programs allow to make a gear that is within the AGMA or ISO quality rating. In fact the standards are already in corporated into many gear design programs. For application where precise tooth profiles are not necessary as in the gear design itself, solid-modeling systems are very useful. Solid modeling is a good

downstream tool, good for defining tool paths for EDMs, lasers and other systems that can draw data from CAD systems. Solid modeling is also the basis for stereo lithography and other rapid prototyping systems.

These capabilities and applications make modern CAD/CAM systems such as Pro/Engineer very powerful engineering design tool with a great deal to offer for the designer. All of this flexibility is possible by the process called parametric modeling [29,30].

### **4.3 What is Pro/Engineer?**

Pro/Engineer is a powerful program that is used to create virtually unlimited range of products with a great precision. The major front-end module of Pro/E is used for part and assembly design and model creation and production engineering drawings. There is wide range of additional modules available to handle tasks ranging from sheet metal operations, piping layout, mold design, numerically controlled machining and other functions. In a nutshell Pro/Engineer is feature based, bi-directional and parametric nature solid modeling system.

#### **4.3.1 Feature-Based Nature of Pro/Engineer**

Pro/Engineer is feature-based solid modeling tool. A feature is defined as the smallest building block and any solid model created in Pro/Engineer is an integration of these building blocks. Each feature can be edited individually to bring in any change in the solid model. The use of the feature-based property provides greater flexibility to the parts Pro/Engineer created.

#### **4.3.2 Bi-Directional Associative Nature of Pro/Engineer**

There is a bi-directional associativity between all modes of Pro/Engineer, this indicates the ability of the software package to ensure that if any modifications are made in particular model in one mode, the corresponding modifications are also reflected in the same model in other modes.

### **4.3.3 Parametric Nature of Pro/Engineer**

Pro/Engineer is parametric in nature, which means that the features of the part become interrelated if they are drawn by taking the reference of each other. You can redefine the dimensions or the attributes of a feature at any time. The changes will propagate automatically throughout the model. Thus, they develop a relationship among themselves. This relationship is known as the parent-child relation. So if someone wants to change the placement of the child feature, he can make alteration in the dimensions of the references and hence change the design as per his requirement.

Parametric modeling allows the design engineer to let the characteristic parameters of a product drive the design of that product. During the gear design, the main parameters that would describe the designed gear such as module, pressure angle, root radius, and tooth thickness... could be used as the parameters to define the gear. But, the parameters do not have to be only geometric. They can also be key process information such as case hardening specifications, Quality of grades, metallurgical properties and even load classifications for the gear being designed.

Pro/Engineer use these parameters, in combination with its features to generate the geometry of the gear and all essential information to create the model. For example, the parametric dimensional values make the shape of the tooth profile and non-geometric parameters information specifies things like the required case hardening depth or non-destructive testing requirements.

An important aspect of feature based modeling in Pro/Engineer is the concept of parent/child relationships. A child feature is one of those references previously created parent feature. For example, the surface of a block might be used as a reference plane to create a slot. A change to the parent feature will also potentially affect the child [29,30].

#### **4.4 Modeling Involute Gears in Pro/Engineer**

The Pro/Engineer user who desires to design a gear should start with the basics: the involute curve. An involute is described as the path of a point on a straight line called the generatrix, as it rolls along the convex base curve (the evolute). The involute curve is most often used as the basis for the profile of a gear tooth.

While several techniques can be used to create the involute tooth profile in Pro/Engineer, this article focuses on using datum curves by equation. The benefits of this method are that the involute curve profile is based on the exact geometric equations, it is highly flexible in terms of the types of gears and curves that can be created. In addition, the datum curve equation method allows the user to use either Cartesian or cylindrical coordinate systems to create the involute profile. Finally, the curves generated by this approach are automatically truncated at the major diameter of the gear without any additional operation [11].

#### **4.5 General Procedures to Create an Involute Curve**

The sequence of procedures employed to generate the involute curve are illustrated as follows: -

1. Set up the geometric parameters
  - ❖ Number of teeth
  - ❖ Diametral Pitch
  - ❖ Pressure angle
  - ❖ Pitch diameter
  - ❖ Face width
  - ❖ Helix angle
2. Create the basic geometry such as addendum, dedendum and pitch circles in support of the gear tooth.
3. Define the involute tooth profile with datum curve by equation using cylindrical coordinate system.
4. Create the tooth solid feature with a cut and extrusion. Additional helical datum curves are also required in this step to sweep helical gear teeth.
5. Pattern the tooth around the centre line axis.

The key specifications of geometrical parameters and the helical gear model developed by using the above procedures in Pro/Engineer are shown in and Table 4.1 and Figure 4.1 respectively.

Table 4.1 key geometrical parameters of helical gear used

Number of teeth	28
Diametral pitch ( p) [mm]	152.4
Pressure angle	25 degree
Face width [mm]	25.4
Addendum [mm]	1/p
Dedendum [mm]	1.25/p
Helix angle	20 degree

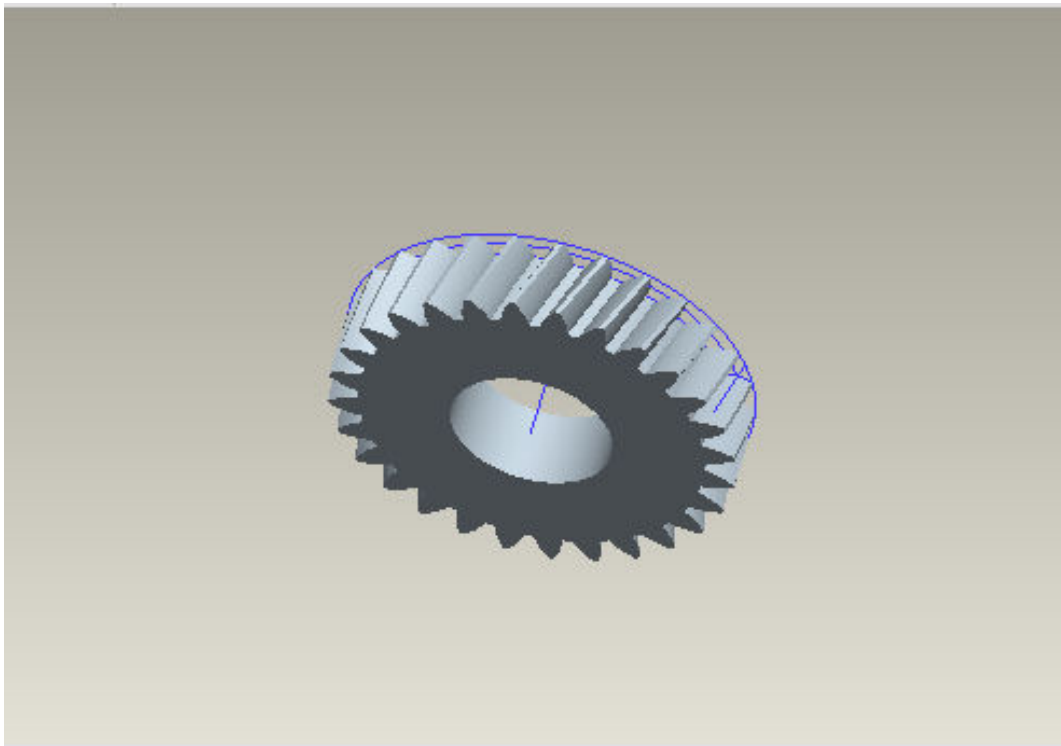


Figure 4.1 solid model of helical gear generated by Pro/Engineer

#### **4.6 FEM Package**

ANSYS is the name commonly used for ANSYS mechanical, general-purpose finite element analysis (FEA) computer aided engineering software tools developed by ANSYS Inc. ANSYS mechanical is a self contained analysis tool incorporating pre-processing such as creation of geometry and meshing, solver and post processing modules in a unified graphical user interface. ANSYS is a general-purpose finite element-modeling package for numerically solving a wide variety of mechanical and other engineering problems. These problems include linear structural and contact analysis that is non-linear. Among the various FEM packages, in this work ANSYS is used to perform the analysis [15].

The following steps are used in the solution procedure using ANSYS

1. The geometry of the gear to be analyzed is imported from solid modeler Pro/Engineer in IGES format this is compatible with the ANSYS.
2. The element type and materials properties such as Young's modulus and Poisson's ratio are specified.
3. Meshing the three-dimensional gear model. Figure 4.2 shows the meshed 3D solid model of gear.
4. The boundary conditions and external loads are applied.
5. The solution is generated based on the previous input parameters.
6. Finally, the solution is viewed in a variety of displays.

## Chapter 5

### Involute Gear Tooth Bending and Contact Stress Analysis

#### 5.1 Introduction

There are many types of gear failures when some one analyzes actual gear in services however; these failures are categorized in two general groups. One is the failure of the root of the teeth when the bending strength is inadequate and the other is created on the surface of the gear. There are two theoretical formulas, which deal with the above two fatigue failure problems. One is the Lewis formula that is used to calculate the bending stress and Hertzian equation that is used to compute the contact stress. Various researchers are used variety of method to determine these stresses. The finite element method is very often used to analyze the state of stress in elastic bodies, which have complicated geometry like gears.

In this Chapter, the bending and contact stresses of helical gear are studied by using the finite element method (ANSYS) and the results are compared with the modified Lewis, which is recommended by AGMA and Hertzian theoretical equation respectively.

#### 5.2 Analytical Bending Stress Analysis

The bending stress is one of the crucial parameters during the analysis of helical gears. When the total repetitive load acting on the gear tooth is greater than its strength then the gear tooth will fail in bending. Bending failure in gears is predicted by a formula developed by Wiltred Lewis [9]. The formula uses the bending of cantilever beam to simulate the bending stress acting on the gear as shown in Figure 5.1, the tangential load ( $F_t$ ) induces bending stress which tends to break the tooth. The maximum bending stress induced by this force is given by

$$\sigma_b = \frac{M C}{I} \dots\dots\dots (5.1)$$

- Where
- M = Maximum bending moment =  $F_t l$
  - $F_t$  = Tangential load acting at the tooth
  - l = Length of the tooth
  - C = Half thickness of the tooth ( $t$ ) =  $t / 2$

$$I = \text{Moment inertia} = \frac{bt^3}{12}$$

b = Width of gear face

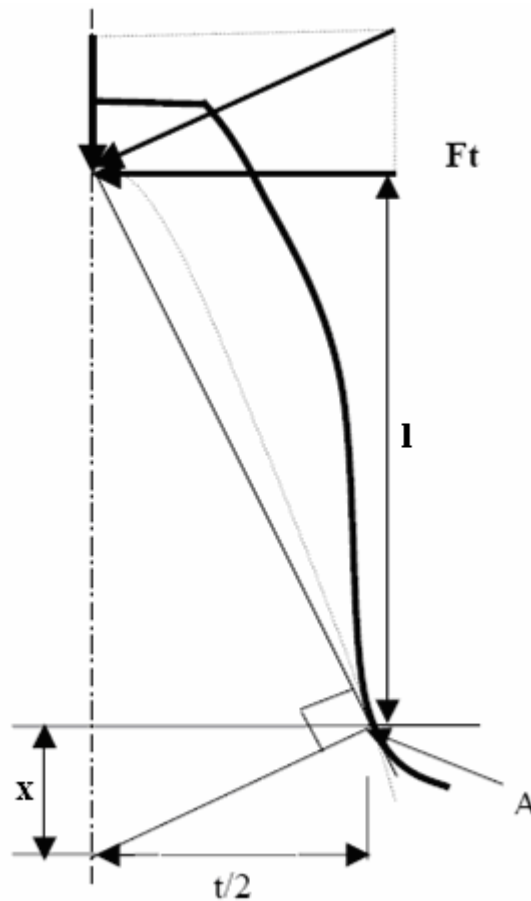


Figure 5.1 the cross section and the dimensions of gear tooth profile to determine the Lewis formula

Substituting the values for M, C and I in equation (5.1) the stress will be

$$\sigma_b = \frac{6F_t \ell}{bt^2} \dots\dots\dots (5.2)$$

From similarity of the two triangles which is shown in Figure 5.1,

$$\frac{t/2}{x} = \frac{\ell}{t/2} \quad \text{This implies} \quad \ell = \frac{t^2}{4x} \dots\dots\dots (5.3)$$

Substituting equation (5.3) into (5.2) and multiplying by a term  $\frac{P_d}{P_d}$  we get,

$$\sigma_b = \frac{3F_t}{2bx} = \frac{3F_t P_d}{2 b p_d x} = \frac{F_t P_d}{b Y} \dots\dots\dots (5.4)$$

Where,  $P_d$  = diametral pitch

$$Y = \frac{2}{3} \times p_d$$

Equation (5.4) is known as Lewis equation, which considers only static loading and doesn't take the dynamics of meshing teeth into account. The above stress formula must be modified to account different situations like stress concentration and geometry of the tooth. Therefore, Equation (5.5) that is shown below is the modified Lewis equation recommended by AGMA for practical gear design to account for variety of conditions that can be encountered in service.

$$\sigma_b = \frac{F_t}{m_n b J} \frac{k_a k_s k_m}{k_v} \dots\dots\dots (5.5)$$

- Where,  $k_a$  = Application factor
- $k_s$  = Service factor
- $k_v$  = Velocity factor
- $F_t$  = Tangential load
- $m_n$  = Normal module
- $J$  = Geometry factor
- $k_m$  = Load distribution factor

Each of these factors can be obtained from machine design books [22]. This analysis considered only the component of the tangential force acting on the tooth and doesn't considered the effects of the radial force, which will cause in compressive stress over the cross section on the root of the tooth. Suppose that the greatest stress occurs where the force is exerted at the top of the tooth, usually there are at least two pairs in contact. In fact, the minimum stress at the root of the tooth occurs when the contact point moves near the pitch circle because there is only one tooth pair in contact and these teeth pairs carries the entire torque or load. When the load is moving at the top of the tooth, two teeth pairs share the whole load if the ratio is longer than one and less than two.

If one tooth pair is considered to carry the whole load and it acts on the top of the tooth, this loading condition is enough to analyze the gear bending stress.

### 5.3 FEM Bending Stress Analysis

In this section, the teeth bending stress of helical gear is calculated using ANSYS. For this purpose the modeled gear in Pro/Engineer is exported to ANSYS as an IGES file and then an automatic mesh is generated. Figure 5.2 shows the meshed three-dimensional model. Figure 5.3 demonstrate the Von Mises stress on the root of the tooth for 28 numbers of teeth helical gear. There are more detailed results for various numbers of teeth in Table 5.3 at section 5.4 which are compared with the result obtained from the Lewis formula.

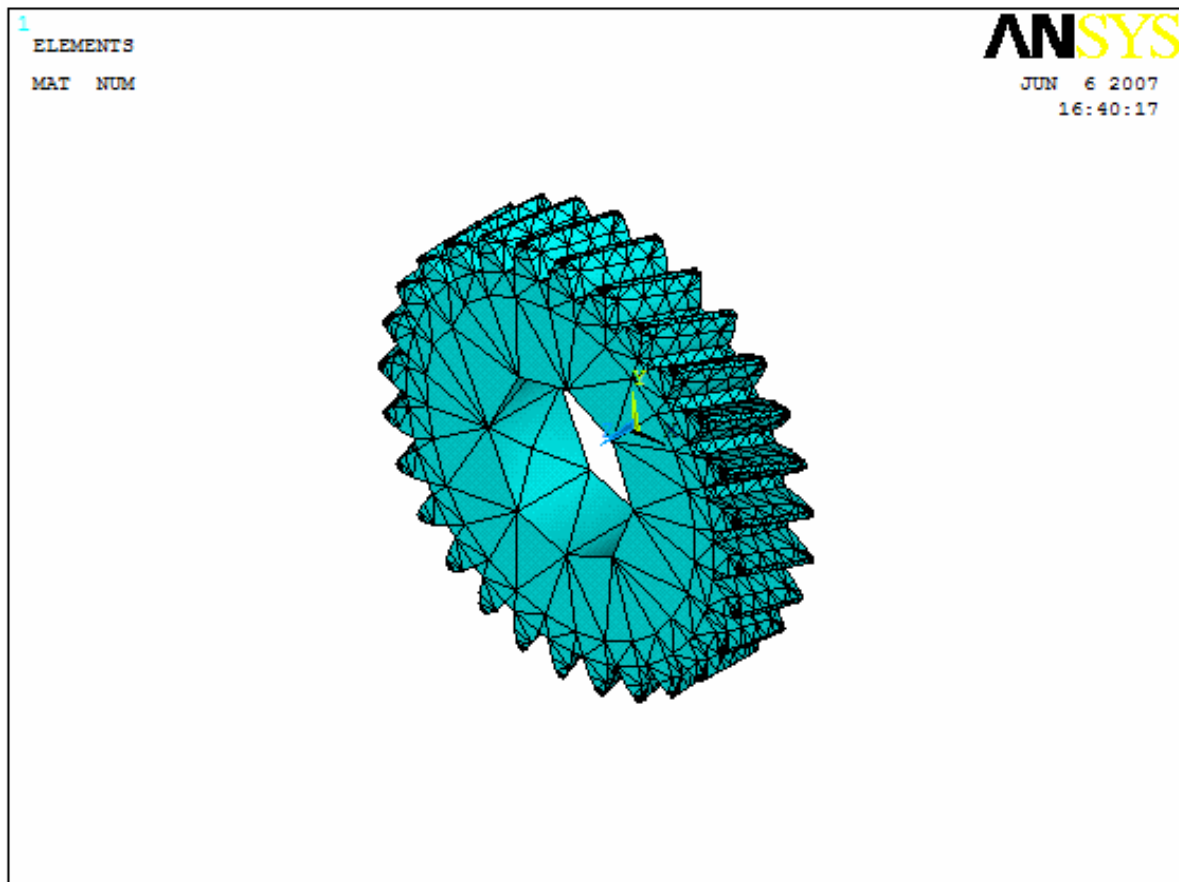


Figure 5.2 Three-dimensional FEM model with 28 teeth

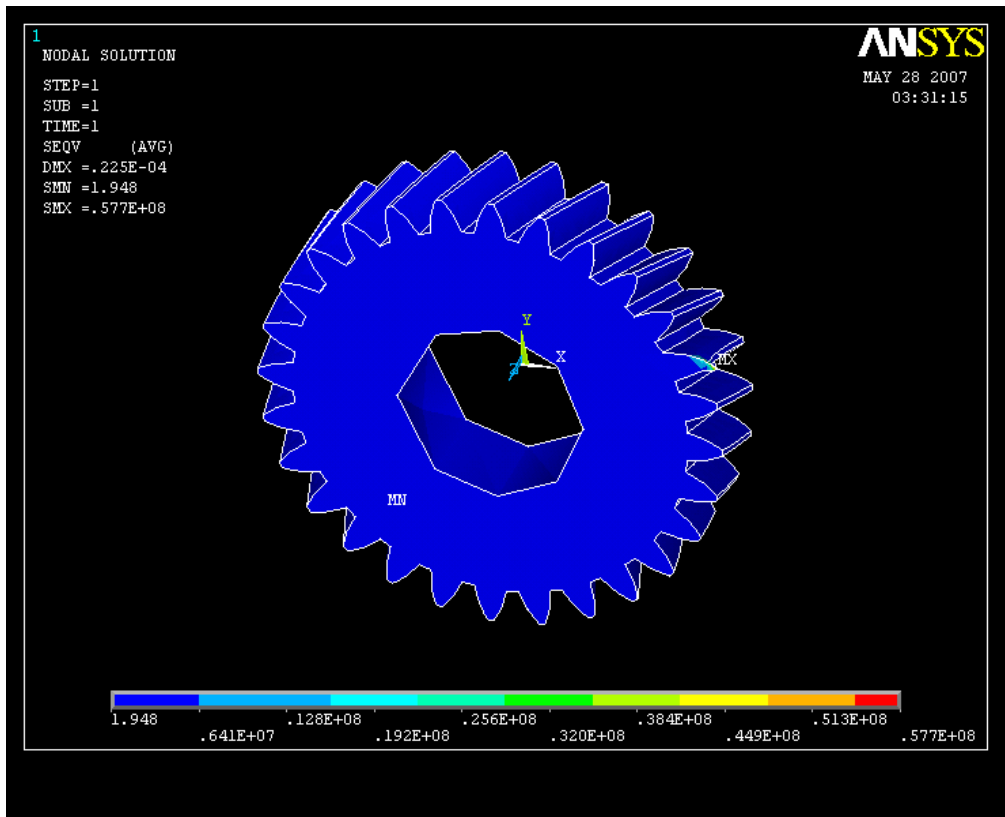


Figure 5.3 Von Mises stress of 28 number teeth modeled gear

The stress distribution which is shown in Figure 5.3 are Von Mises stresses. They are equal to tensile stresses; these tensile stresses are the main cause of crack failure if they are greater than the strength of the tooth. That is why cracks usually start from the tensile side. From the Lewis equation if the diameter of the pinion and the gear are kept constant and the number of teeth is changed then the diametral pitch and the module of the gear will be changed that means there are different bending strength between various numbers of teeth. Different maximum Von Mises stresses with various numbers of teeth are shown in Table 5.1.

Table 5.1 Maximum bending stresses (Von Mises) obtained from ANSYS

Number of teeth	Load [N/MM]	Maximum bending stress (ANSYS) [Mpa]
20	287.75	61.44
25	287.75	59.63
28	287.75	57.70
30	287.75	57.07
37	287.75	56.86

#### 5.4 Comparison of Results using AGMA Bending Stress Formula

In this section, the bending stresses obtained from the analysis of the three-dimensional model using ANSYS is compared with the calculated values from the standard recommended by AGMA during the design of helical gears. Equation (5.5) the modified Lewis equation suggested by AGMA is used to get the corresponding results. Here the analysis is carried out with different number of teeth. In this calculation except the geometric factor ( $J$ ) all other coefficients ( $k_a, k_s, k_m$  &  $k_v$ ) are taken as unity [3], geometric parameters of the gear and the applied load are assumed to be constant. The maximum bending stresses resulted from this analytical solutions together with the tooth geometric factor are tabulated in table 5.2.

Table 5.2 bending stress from AGMA formula

Number of teeth (N)	Geometric factor (J) [22]	Maximum Bending Stress using AGMA Formula Eq. (4.5) in Mpa
20	0.5000	60
25	0.5300	57.04
28	0.5400	55.98
30	0.5500	54.97
37	0.5625	53.74

To verify the result obtained from ANSYS it is compared with the value calculated from AGMA formula. The maximum difference between these two outcomes is 5.49%, therefore the developed FEA models are good enough for the stress analysis.

Table 5.3 Comparisons of maximum bending stresses

Number of Teeth	$\sigma_{(AGMA)}$ [Mpa]	$\sigma_{(ANSYS)}$ [Mpa]	Differences [%]
20	60	61.44	2.35%
25	57.04	59.63	4.34%
28	55.98	57.70	2.98%
30	54.97	57.07	3.68%
37	53.74	56.86	5.49%

### 5.5 Contact Stress Analysis

One of the main gear tooth failure is pitting which is a surface fatigue failure due to many repetition of high contact stresses occurring in the gear tooth surface while a pair of teeth is transmitting power. Contact failure in gears is currently predicted by comparing the calculated Hertz contact stress to experimentally determined allowable values for the given material. The method of calculating gear contact stress by Hertz's equation originally derived for contact between two cylinders. Contact stresses between cylinders are shown in Figure 5.4, in this figure an ellipsoidal-prism pressure distribution is generated between the two contact areas.

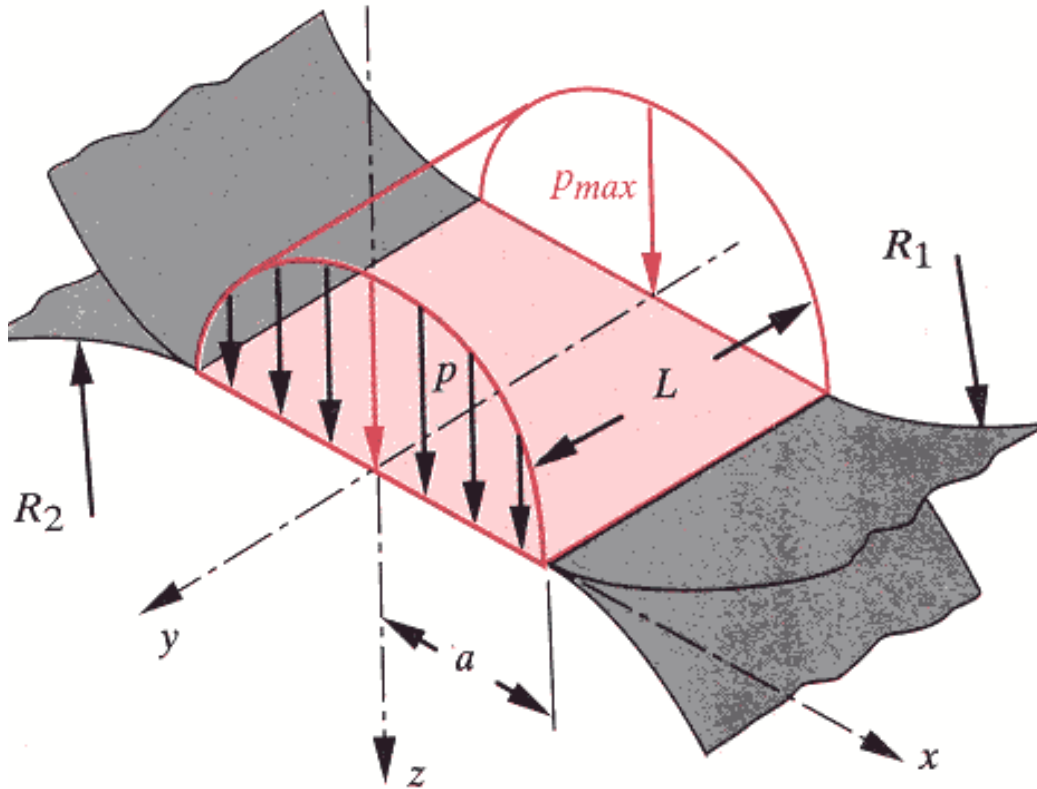


Figure 5.4 Ellipsoidal –prism pressure distribution

From figure 5.4 the width of the contact zone is  $2a$ . If the total contact force is  $F$  and contact pressure is  $p(x)$ , there is a formula [3] which illustrates the relationship between the force  $F$  and the pressure  $p(x)$  :

$$F = 2L \int_0^a p(x) dx \dots\dots\dots (5.6)$$

$$\text{Contact width } a = \sqrt{\frac{2F \left( \frac{1-\nu_1^2}{E_1} + \frac{1-\nu_2^2}{E_2} \right)}{\pi L \left( \frac{1}{d_1} + \frac{1}{d_2} \right)}} \dots\dots\dots (5.7)$$

$$\text{The maximum contact stress is given } P_{\max} = \frac{2F}{\pi a L} \dots\dots\dots (5.8)$$

Where  $d_1$  and  $d_2$  represent the pinion and gear pitch diameters. Therefore the maximum surface (Hertz) stress becomes:

$$P_{\max} = \sigma_H = 0.564 \sqrt{\frac{F \left( \frac{1}{R_1} + \frac{1}{R_2} \right)}{\frac{1-\nu_1^2}{E_1} + \frac{1-\nu_2^2}{E_2}}} \dots\dots\dots (5.9)$$

F is load per unit width,

$R_i$  = is the radius of cylinder,  $R_i = d_i \sin \varphi / 2$  for the gear teeth,

$\varphi$  = is pressure angle,  $\nu_i$  = is poisson's ratio for cylinder i,

$E_i$  = is Young's modulus for cylinder i.

### 5.6 Numerical Example of Contact Stresses between two Circular Cylinders

Despite the importance of contact analysis in solid mechanics contact effects are rarely seriously taken into account in conventional engineering analysis because of difficulties and extreme complexity involved during modeling and solution. To over come these modeling and solution difficulties and to examine the contact stresses in gears, two circular elastic discs under two-dimensional contact are analyzed and the numerical solutions are compared with that of the Hertz theory contact stress formula.

Consider two circular cylinders with  $R_1=R_2=76.2\text{mm}$  as shown in figure 5.5. Half of the cylinders are divided into the finite element mesh to reduce the number of nodes and elements to save computer memory space and time to solve. This model is built based on the Hertz contact stress theoretical problem the radius is calculated from the pitch diameters of the pinion and the gear and other parameters are shown in table 5.4 and figure 5.5.

Table 5.4 parameters of helical gear used

Number of teeth	25
Normal Module (M)	6 mm
Normal pressure angle	20 degrees
Face width (mm)	0.015M
Addendum (mm)	1.00M
Dedendum (mm)	1.25M
Helix angle	20 degrees

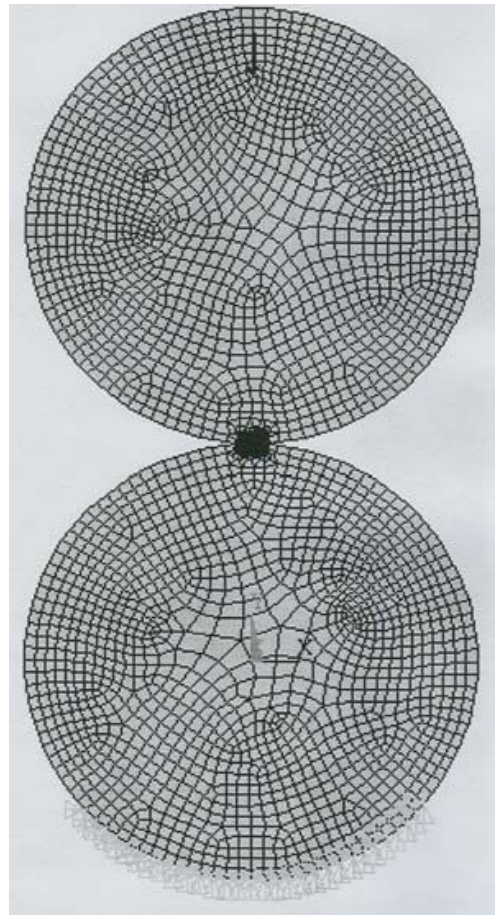
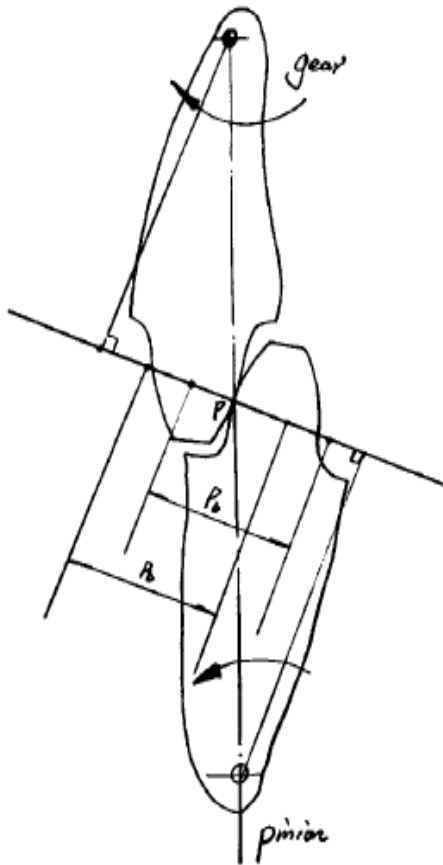


Figure 5.5 two steel cylinders pressing against each other

In this model two cylinders are pressed against to each and the contact stresses of this model represent the contact stress between two gears. To solve the problem in ANSYS, the geometry of the two half cylinders is defined then meshed.

Around the contact areas fine mesh is built. After that the boundary conditions are applied in the model. Finally the loads are applied (Figure 5.6). The steel is used in this problem have materials properties elastic modulus of 207Gpa and poisson's ratio 0.3.

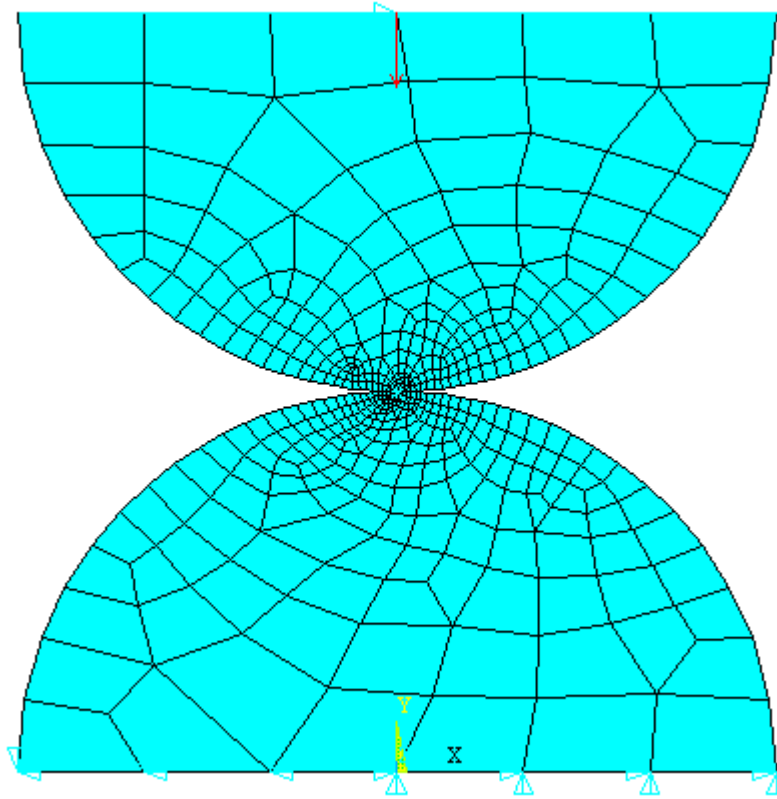
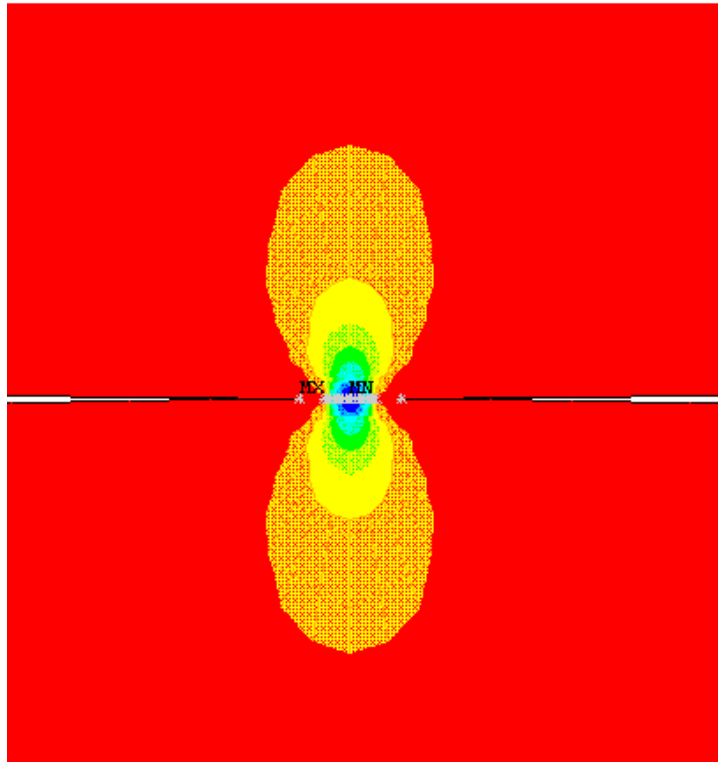


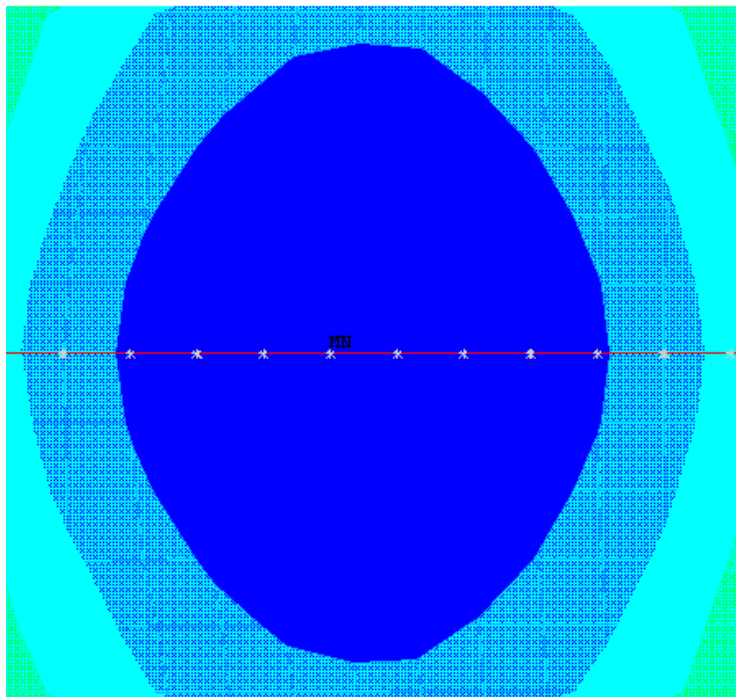
Figure 5.6 loading, boundary condition and meshing of half of the cylinders

### 5.7 Results and Comparison of the Contact Stresses Analysis

After applying the load with magnitude 500N, the model is analyzed to get the contact stresses. The normal contact stress along with the contact surface from ANSYS is shown in Figure 5.7. Figure 5.7(a) and 5.7(b) show the distributions of this stress along with the contact area.



(a)



(b)

Figure 5.7 the distribution of normal contact stress along the contact area

Figure 5.8(a) and (b) show the maximum shear stresses. The subsurface location of the maximum shear stress can be seen also lying below the surface at the centre of the contact zone, which is shown in Figure 5.8 (b) the location is designated by with labels MX and MN, since the two contact cylinder are made of steels the maximum shear stress occurs at a depth of  $0.786a$  where  $a$  is half of the contact length shown in Figure 5.4 and its magnitude is about  $0.304P_{\max}$  [3].

Figure 5.9 (a) and (b) under the contact areas show orthogonal shear stress. The largest orthogonal shear stress lies below the surface at the edge of the contact region that is shown in Figure 5.9 (b). The subsurface location of maximum shear stress is believed to be an important factor in surface fatigue failure. The theory of gearing indicates that cracks that begin below the surface eventually grow to the point that the material above the crack breaks out to form a pit.

The next step is to compare results from ANSYS with the values obtained from the Hertz theoretical equation. For the contact geometry that is shown in Figure 5.4, the maximum Hertz contact stress is given by equation 5.9 the other forms of stresses due to the normal loading  $F_{\max}$  are given by [3]:

$$\sigma_x = -\frac{y}{\pi} \left[ \frac{a^2 + 2x^2 + 2y^2}{a} \beta - \frac{2\pi}{a} - 3x\alpha \right] F_{\max} \dots\dots\dots(5.10)$$

$$\sigma_y = -\frac{y}{\pi} [a\beta - xa] F_{\max} \dots\dots\dots(5.11)$$

$$\tau_{xy} = -\frac{1}{\pi} y^2 \alpha F_{\max} \dots\dots\dots(5.12)$$

Where the factors  $\alpha$  and  $\beta$  are given by

$$\alpha = \frac{\pi}{k_1} \frac{1 - \sqrt{\frac{k_2}{k_1}}}{\sqrt{\frac{k_2}{k_1}} \sqrt{2\sqrt{\frac{k_2}{k_1}} + \left( \frac{k_1 + k_2 - 4a^2}{k_1} \right)}} \dots\dots\dots(5.13)$$

$$\beta = \frac{\pi}{k_1} \frac{1 + \sqrt{\frac{k_2}{k_1}}}{\sqrt{\frac{k_2}{k_1} \sqrt{2\sqrt{\frac{k_2}{k_1}} + \left(\frac{k_1 + k_2 - 4a^2}{k_1}\right)}}} \dots\dots\dots (5.14)$$

$$k_1 = (a + x)^2 + y^2$$

$$k_2 = (a - x)^2 + y^2 \dots\dots\dots (5.15)$$

But these above equations are not used to calculate the stresses on the surface because if we set y=0, then the result in the stresses being calculated become zero. Therefore, for comparison the equivalent peak values of stresses such as maximum normal stress, the maximum shear stress and the maximum orthogonal shear stress are calculated from the maximum Hertz stress (equation 5.9) as follow [3].

$$\sigma_x = \sigma_z = -P_{max} \dots\dots\dots (5.16)$$

$$\sigma_{y(normal)} = -2\nu P_{max} \dots\dots\dots (5.17)$$

$$\sigma_{Von Mises} = 0.57 P_{Max} \dots\dots\dots (5.18)$$

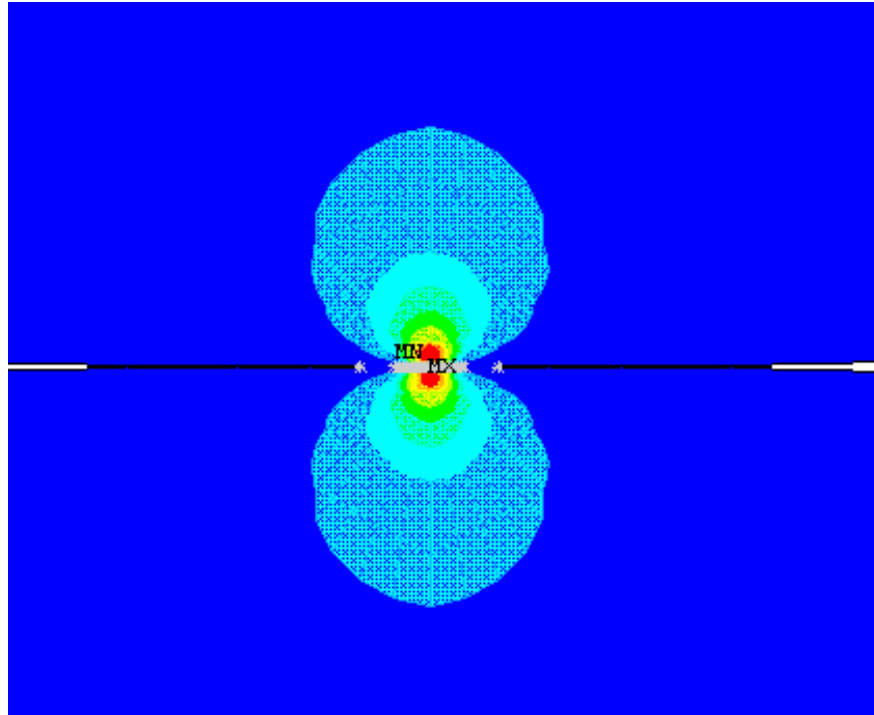
$$\tau_{Max shear} = 0.304 P_{Max} \dots\dots\dots (5.19)$$

$$\tau_{Orthogonal shear} = 0.25 P_{Max} \dots\dots\dots (5.20)$$

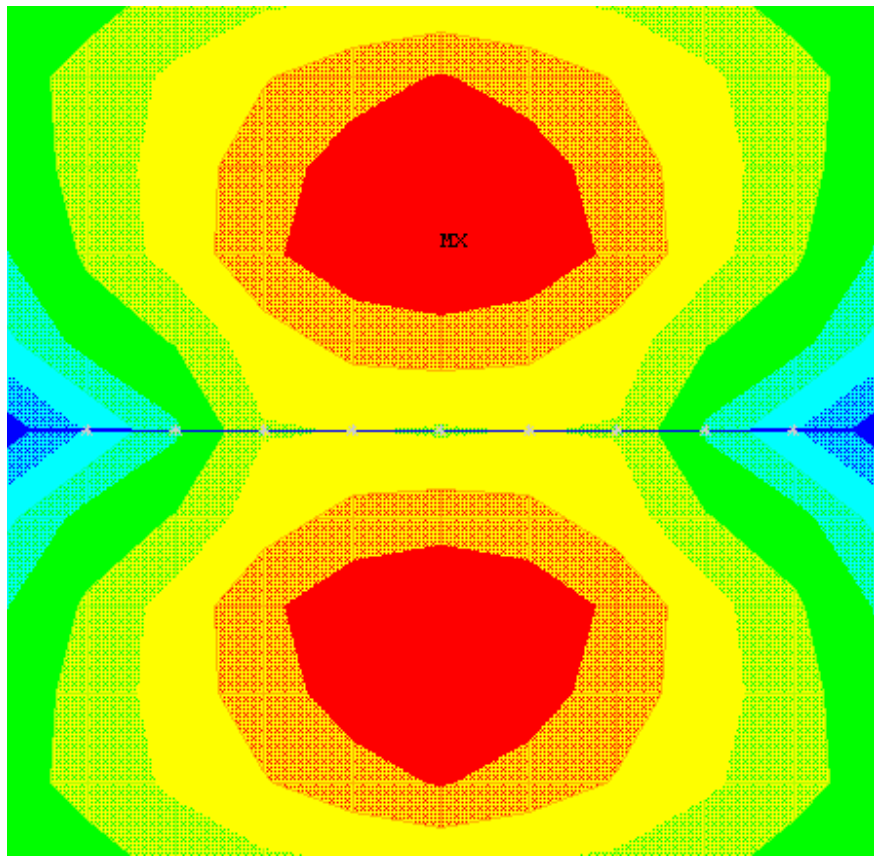
Where  $P_{Max} = \sigma_H$  which is the maximum Hertz stress. The results obtained from these equations are compared with FEM (ANSYS) values and verified in the following table.

Table 5.5 Comparison of peak values of the equivalent stresses

Types of stress	Helix angle ( $\beta$ ) [Degree]	Calculated Hertezian stress [Mpa]	ANSYS value [Mpa]	Differences [%]
$\sigma_{Normal}$	15	83.05	80.95	2.53%
	20	82.2	79.02	3.86%
	25	80.76	79.56	1.46%
$\tau_{Max shear}$	15	44.12	45.34	2.69%
	20	41.55	42.12	1.36%
	25	40.05	40.78	1.79%
$\tau_{orthogonal shear}$	15	36.00	36.93	2.51%
	20	34.17	35.21	2.95%
	25	33.48	34.02	1.59%

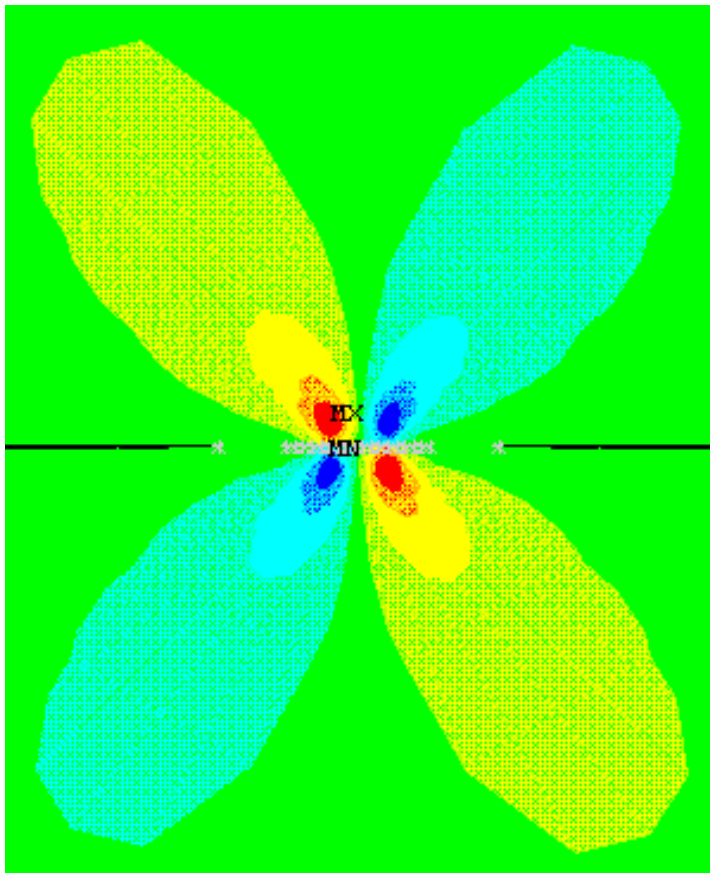


(a)

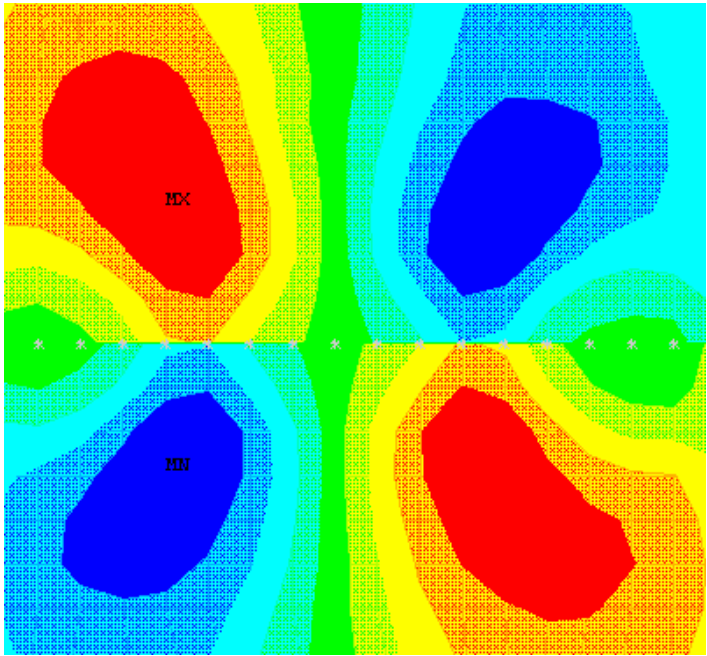


(b)

Figure 5.8 the distribution of maximum shear stress from ANSYS



(a)



(b)

Figure 5.9 the distribution of orthogonal shear stress from ANSYS

## 5.8 Parametric Study

In this section the modeled helical gear (Figure 4.1) is analyzed to study the effect of face width and helix angle on the maximum bending stress under static load with different parameters. Among the various key geometrical parameters which are mentioned in Table 4.1, this section discusses the effect of face width and helix angle. Throughout the analysis each gear is studied for five different face widths

(  $b=80.4\text{mm},60.4\text{mm},45.4\text{mm},35.4\text{mm},25.4\text{mm}$ ) and five helix angles

(  $\beta =15^{\circ},20^{\circ},25^{\circ},30^{\circ},35^{\circ}$ ) all the rest parameters and the applied load are kept constant.

## 5.9 Results and Discussions

The maximum bending stress obtained from ANSYS of the modeled gear for various number of teeth, face width ( $b$ ) =25.4mm and helix angle ( $\beta$ ) =20<sup>0</sup> which is shown in Figure5.3 has been compared in Table 5.3 with the value calculated from AGMA formula (equation5.5).the results obtained from the parametric study of the face width and helix angle will be shown below.

### 5.10 Effect of Face Width

The effect of face width on maximum bending stress is studied by varying the face width for five different values which are (  $b=80.4\text{mm},60.4\text{mm},45.4\text{mm},35.4\text{mm},25.4\text{mm}$ ).The magnitude of the stresses obtained for these face widths are displayed below in Table 5.6.

Table 5.6 Effect of face width on maximum bending stress

Face Width [mm]	$\sigma_{(AGMA)}$ [Mpa]	$\sigma_{(ANSYS)}$ [Mpa]	Differences [%]
80.4	17.69	17.88	1.06%
60.4	23.54	23.84	1.25%
45.4	31.32	31.92	1.88%
35.4	40.17	42.20	2.50%
25.4	55.98	57.70	2.98%

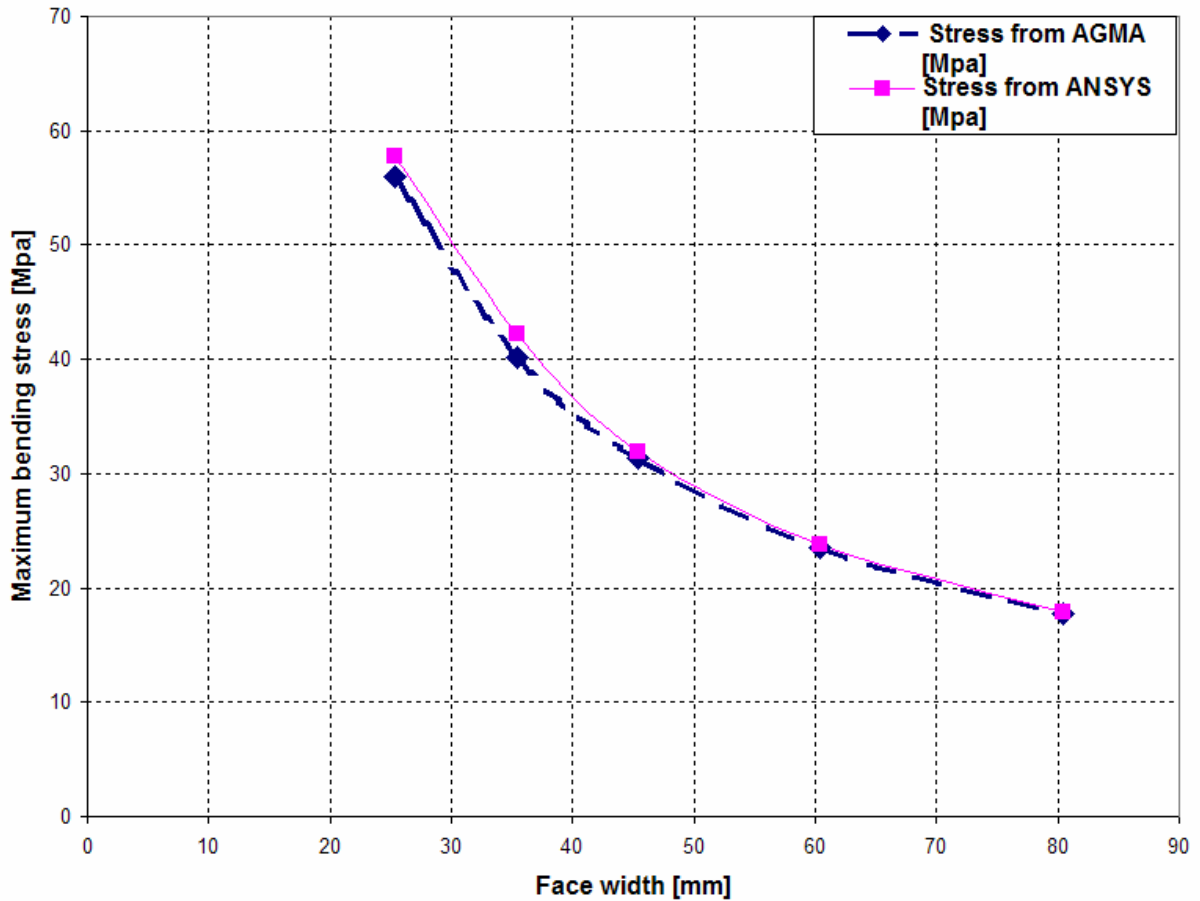


Figure 5.10 graphical representation of Effect of face width on maximum bending stress

As it is seen clearly from the above Table and the Figure 5.10 the maximum bending stress values are increase with the decrease of face width.

### 5.11 Effect of Helix Angle

In this part of the work, apart from the constant number of teeth, module and pressure angle. The face width is also kept constant ( $b=25.4\text{mm}$ ) and the helix angle is varied from  $15^\circ$  to  $35^\circ$  in steps of  $5^\circ$ . The maximum bending stresses obtained are shown in Table 5.7 and it is observed from the Figure 5.11 there is a variation in the maximum bending stresses with the change in helix angle. The maximum bending stress value decreases with the increase of helix angle which is in close agreement with values obtained from AGMA formula.

Table5.7 Effect of helix angle on maximum bending stress

Helix Angle ( $\beta$ )	$\sigma_{(AGMA)}$ [Mpa]	$\sigma_{(ANSYS)}$ [Mpa]	Differences [%]
15 <sup>0</sup>	56.94	58.17	2.11%
20 <sup>0</sup>	55.98	57.70	2.98%
25 <sup>0</sup>	53.14	54.87	3.15%
30 <sup>0</sup>	49.95	52.33	4.54%
35 <sup>0</sup>	44.68	47.07	5.02%

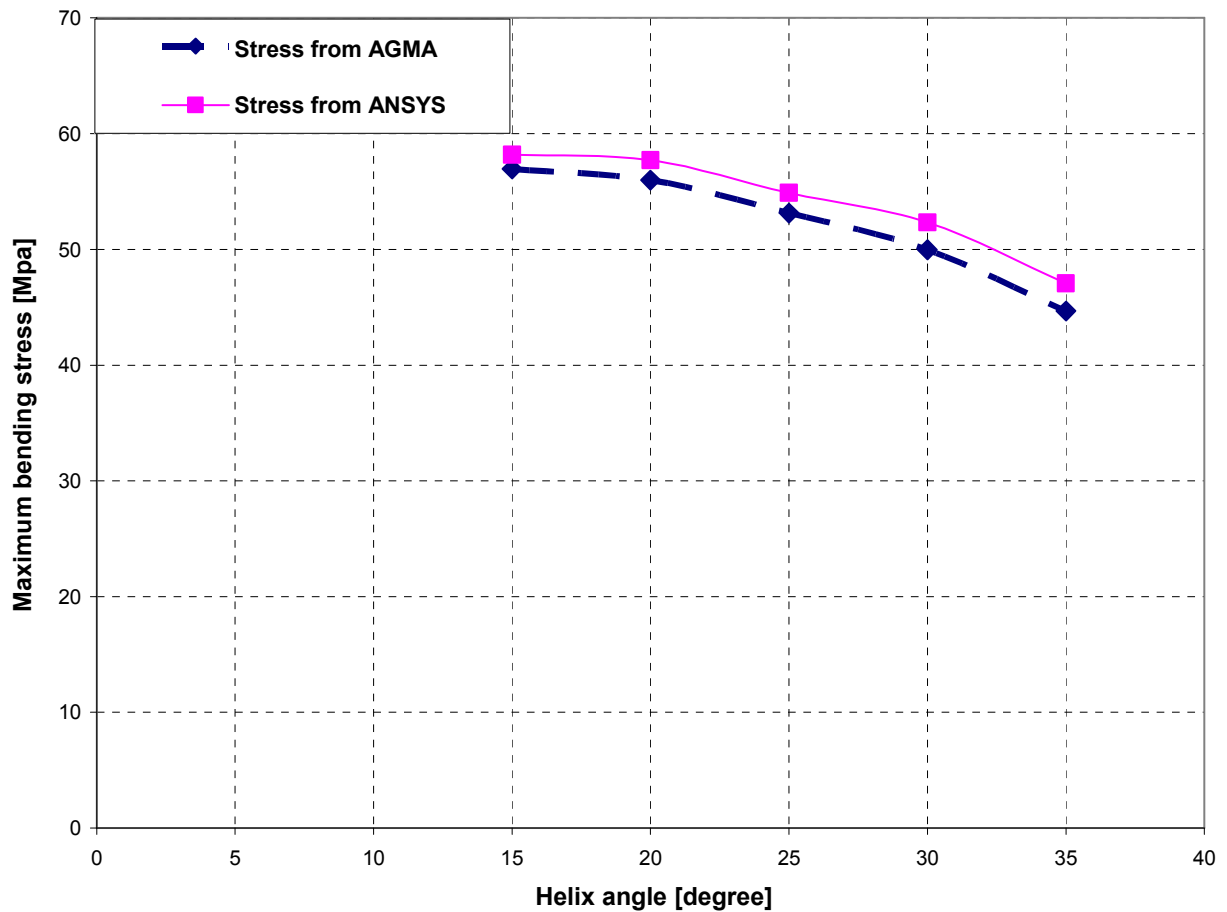


Figure 5.11 graphical representation of effect of helix angle on maximum bending stress

### 5.12 Combined Effect of the Face Width and Helix Angle

On the other hand to analyze the effect of both the face width and the helix angle, the maximum stress values obtained which is shown in Table 5.6 and 5.7 are tabulated in Table 5.8 and plotted in Figure 5.12 to get the overall idea of how the maximum bending stresses vary with different face widths and helix angles. It is observed from the Table 5.8 and Figure 5.12 for the gears of helix angle greater than  $15^{\circ}$ , there is a decrease in the maximum bending stress values with the increase helix angle, for gears of smaller face width and this decrease in maximum bending stress values is smaller in the case of gears having larger face width.

Table 5.8 the combined effect of face width (b) and helix angle ( $\beta$ )

Face width [mm]	Maximum Bending Stress [Mpa]				
	$\beta = 15^{\circ}$	$\beta = 20^{\circ}$	$\beta = 25^{\circ}$	$\beta = 30^{\circ}$	$\beta = 35^{\circ}$
25.4	58.17	57.70	54.87	52.33	70.11
35.4	43.05	41.20	40.33	37.26	50.31
45.4	32.46	31.92	30.25	27.85	39.23
60.4	24.10	23.84	22.43	20.63	29.48
80.4	18.02	17.88	16.79	15.45	13.61

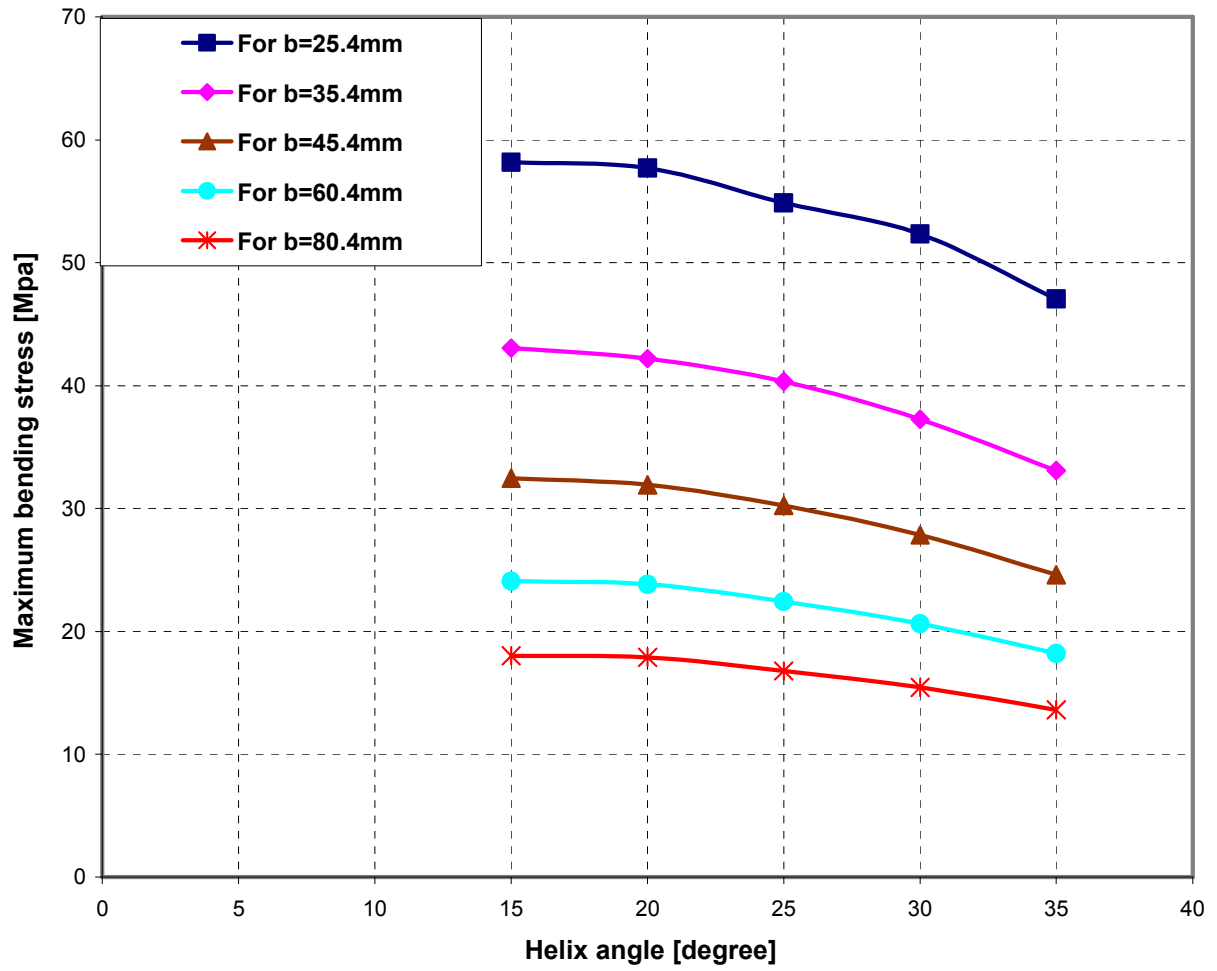


Figure 5.12 graphical representation of the combined effect of face width (b) and helix angle ( $\beta$ ) along the face width

## Chapter 6

### Conclusion and Future Work

#### 6.1 Conclusion

Analytical method of gear analysis uses a number of assumptions and simplifications and it is intended to determine the maximum stress values. In this paper, numerical approach has used for predicting the static contact and bending stresses of involute helical gear. A parametric study is also made by varying the face width and helix angle to investigate their effect on the bending stress of helical gears. The contribution of this thesis work can be summarized as follows:

The strength of the gear tooth is a crucial parameter to prevent failure. In this study, it is shown that the effective method to estimate the root bending stresses using three dimensional model of the gear and to verify the accuracy of this method the results with different number of teeth are compared with the standard formula.

It is also shown that the development of finite element analysis model of the equivalent contact cylinders to simulate the contact stress between two gears reasonably and the obtained result is compared with the Hertzian theoretical equation.

Based on the result from the contact stress analysis the hardness of the gear tooth profile can be improved to resist pitting failure: a phenomena in which a small particle are removed from the surface of the tooth that is because of the high contact stresses that are present between mating teeth.

The face width and helix angle are an important geometrical parameters during the design of gear. As it is expected, in this work the maximum bending stress decreases with increasing face width and it will be higher on gear of lower face width with higher helix angle. As a result, based on this finding if the material strength value is criterion then a gear with any desired helix angle with relatively larger face width is preferred.

## **6.2 Recommendation and Future work**

This thesis paper can be an interest for researchers, instructors and postgraduate students who have great enthusiasm to work more on gears. It may give enlightenment about the characteristics of involute helical gears and evoke pervious works of various bodies that are involved in gears research and production. Further more this study contribute to a better gear design, assist technological institutions and all those who are interested in involute helical gears. More work can be done to improve this study and to obtain better output. Generally, the following areas are worthy for further research in the light of this thesis.

- ❖ Further three dimensional numerical method of investigation and study can be conducted on the analysis of bending and contact stresses for all types of gears such as spur, bevel and other tooth forms.
- ❖ Further numerical method of investigation and study can be conducted on the whole gearbox with all elements in the system including gear casing and bearing.
- ❖ Further numerical method of investigation and study can be conducted on gears in mesh under dynamic condition with and with out cracked teeth, surface pitting or wear.
- ❖ The bending and contact stress analysis of gears made of composite materials using three-dimensional finite element analyses can be recommended as future work.
- ❖ The contact stress can be reanalyzed for a better result by simulating the real contact region between the two mating gears instead of using the equivalent cylinders by improving the solution in a high capacity computer.

## References

- [1]. Yonatan, F., **Variable Mesh Stiffness of Spur Gear Teeth Using FEM**, M.sc. thesis  
Department of mechanical Engineering, Addis Ababa University
- [2]. Tsay, C.B., and Fong, Z.H., **Computer Simulation and Stress Analysis of Helical Gears with Pinions Circular arc teeth and Gear involute teeth**, Mech. of Mach. Theory, 26, pp.145-154, 1991.
- [3]. Norton, R.L., **Machine Design: An Integrated Approach**, New Jersey: prentice-Hall Inc. 1996.
- [4]. Vijayarangan, S., and Ganesan, N., **A Static Analysis of Composite Helical Gears Using Three-dimensional Finite Element Method**, Computers & Structures, 49,pp.253- 268,1993.
- [5]. Maitra, G.M, **Hand Book of Gear Design**, TataMcGraw-Hill, New Delhi, 2004.
- [6]. Rao, C.M., and Muthuveerappan G., **Finite Element Modeling and Stress Analysis of Helical Gear, Teeth**, Computers & structures, 49,pp.1095-1106, 1993.
- [7]. Singiresu S. Rao “The Finite Element Method in Engineering”.
- [8]. Lu, J., Litivin, F., and Chen, J.S., **Load Share and Finite Element Stress Analysis for Double Circular-Arc Helical Gears**, Mathl.Comput.Modeling, 21,pp.13-30.1995.
- [9]. Orthwein, W.C., **Machine Component Design**, Jauo publishing House, Mumbai, 2004.
- [10]. Jianfeng L., Mingtain, X., and Shouyou, W., **Finite Element Analysis of Cylindrical Gears**, Communication in Numerical Methods in Engineering, 14, pp.963-975, 1998.
- [11]. Condoor, S., **Modeling using pro/Engineer Wildfire 2.0**, SDC, 2004.
- [12]. Litivin, F.L., and Fuentes, A., **Gear Geometry and Applied theory**, Cambridge University Press, Cambridge, 2004.
- [13]. Jianfeng L., Mingtain, X., and Shouyou, W., **Finite Element Analysis of Instantaneous Mesh Stiffness of Cylindrical Gears (with and without flexible Gear body)**, Communication in numerical methods Engineering, 15,pp.579-587, 1999.

- [14]. Tickoo, S, **Pro/engineer Wildfire for Engineers and Designers Release 2.0**, Dream tech, New Delhi, 2005.
- [15]. Marappan, S. and Verkataramana, **ANSYS Reference Guide**, CAD CENTRE, India, 2004.
- [16]. Zhang, J.J., Esat, I.I., Shi, and Y.H., **Load Analysis with Varying Mesh Stiffness**, Computers and Structures, 70,pp.273-280, 1999.
- [17]. Krishaamoorthy, C., **Finite Element Analysis Theory and programming**, TataMcGraw-Hill, New Delhi, 1994.
- [18]. Hwon Y.W., and Bang H., **The Finite Element Method using Matlab**, CRC Press Boca Rotor, USA, 1999.
- [19]. Zhang, Y., and Fang.Z, **Analysis of Tooth Contact and Load Distribution of Helical Gears with Crossed axes**, Mechanism and MachineTheory, 34,pp.41-57, 1999.
- [20]. Coy, J.J., and Townsend, D.P., **Gearing**, NASA Reference Publication 1152, AVSCOM Technical Report 84-C-1 5, 1985.
- [21]. Cheng, Y., and Tsay C.B., **Stress analysis of Helical Gear set with Localized Bearing Contact**, Finite Element in Analysis and Design, 38,pp.707-723, 2002.
- [22]. Shigley, J.E., and Mischke, C.R., **Standard Handbook of Machine Design**, McGraw-Hill, USA, 1996.
- [23]. Litvin, F.L., Fuentes, A., Perez, I.G., L.Carnevali, L., and Sep, T.M., **New version of Novikov-Wildhaber helical gears: “Computerized design, simulation of Meshing and stress analysis**, Computational Methods in applied mechanics and Engineering, 191,pp.5707-5740, 2002.
- [24]. Wagaj, P., and Kahraman, A., **Impact of Tooth Profile Modifications on the Transmission error Excitation of Helical Gear Pairs**, 6th Biennial Conference on Engineering Systems Design and Analysis, Istanbul-Turkey, July 8-11, 2002.
- [25]. Toogood, R., **Pro/Engineer Advanced Tutorial**, SDC publications, Canada, 2000.

- [26]. Vera, N.S., and Ivan, C., **The Analysis of Contact Stress on Meshed Teeth's Flanks along the path of Contact for a tooth pair**, Mechanics Automatic Control and Robotics, 3,pp, 1055-1066,2003.
- [27]. Barone, S., Borgainil, L., and Forte, P., **CAD/FEM Procedure for Stress analysis of in Unconventional Gear Applications**, International Journal of Computer Application in Technology, 15,pp.1-11, 2001.
- [28]. Huston, R.L., Mavriplis, D., Oswald, B.F., and Liu, Y.S., **A Basis for Solid Modeling of Gear Teeth with Application in Design and Manufacturing**, NASA Technical Memorandum 105392,1992.
- [29]. <http://www.geartechnology.com/mag/gt-model.htm>
- [30]. <http://www.geartechnology.com/mag/gt-solid.htm>
- [31]. Park, S., J., and Yoo, W., S., **Deformation Overlap in the Design of Spur and Helical Gear pair**, Finite Elements in Analysis and Design, 40,pp.1361-1378, 2004.
- [32]. Litivin, F., Perez, I.G., Fuentes, A., Vecchiato, D., and Thomas, M.S., **Generalized Concepts of meshing and Contact of involute Crossed Helical Gears and its Application**, Compu. Methods & Appli. Eng., 194,pp.3710-3745, 2005.
- [33]. Hedlund, J., and Lehtovaara, A., **Modeling of Helical Gear Contact with tooth Defection**, Tampere University of Technology, Machine Design, P.o.box 589,33101 Tampere, Finland.
- [34]. Coy, J. J., and Zaretsky, E.V., **Life Analysis of Helical Gear sets using Lundberg-Palmgren Theory**, NASA Technical Notes, NASA TN.D-8045, 1975.
- [35]. Litvin, F.L., Fuentes, A., Perez, I.G., Carnevali, L., and Kawasaki, K., **Modified Involute Helical Gears: Computerized Design, Simulation of Meshing, and Stress Analysis**, NASA/CR-2003-212229.